Chapter 18
Wind Turbine Tribology

Elon J. Terrell, William M. Needelman and Jonathan P. Kyle

18.1 Introduction

Wind power is of increasing interest in society due to its prospects as an environmentally friendly source of renewable energy. The use of wind turbines to extract electrical energy from wind can be dated back to the late-1800s, with the 12 kW windmill generator by Charles Brush [1], as well as the mid-1900s, with the 1250 kW Smith-Putnam wind turbine. Developments in the wind industry were encouraged by the oil crisis in 1973. Between the early developments of wind turbines and the present day, wind turbine designs have made significant developments in complexity, size, and power capacity (Fig. 18.1). Wind power is now recognized as one of the fastest growing source of energy production (Fig. 18.2), having a worldwide wind power installed capacity exceeding 120 GW [2–4]. The future prospects for wind power installation indicate that growth will continue, as the United States Department of Energy targets 20% wind-based electricity generation, i.e. over 300 GW, by 2030 [5], while TPWind predicts wind energy to account for 12–14% of the total energy production by 2020 and 25% by 2030 [6]. Additionally, China aims for 15% renewable power generation by 2020 [7, 8].

E. J. Terrell (✉) · J. P. Kyle
Mechanical Engineering Department, Columbia University,
500 West 120th Street, New York, NY 10027, USA
e-mail: eterrell@columbia.edu

J. P. Kyle
e-mail: jpk2128@columbia.edu

W. M. Needelman
Donaldson Company, Inc, 8 Hillside Court,
Huntington, NY 11743, USA
e-mail: bill.needelman@donaldson.com

M. Nosonovsky and B. Bhushan (eds.), *Green Tribology*,
Green Energy and Technology, DOI: 10.1007/978-3-642-23681-5_18,

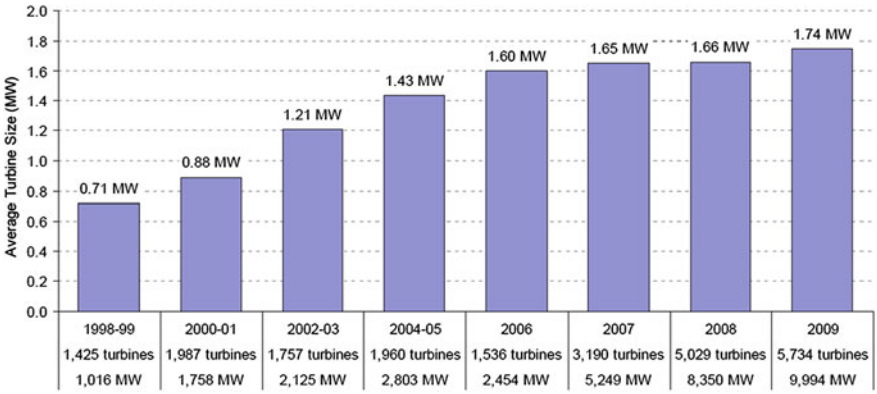

Fig. 18.1 Average nameplate power capacity of installed wind turbines in the united states between 1998 and 2009, from [9]

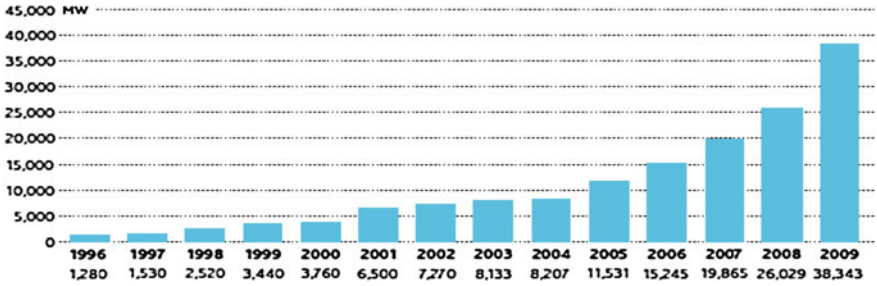

Fig. 18.2 Global annual installed wind capacity between 1996 and 2009, from [4]

Although wind turbines are being increasingly installed around the world, their power systems have a great deal of challenges related to tribology that can drastically reduce their expected lifetimes. Most wind turbines are intended for operating lifetimes of 20 years or longer; however, field reports [10] have shown that drivetrain components tend to fail much earlier than 20 years. These added maintenance and repair costs contribute significantly to the total cost of wind energy [11].

18.2 Wind Energy Siting and Maintenance Costs

Wind energy projects may be on land or offshore, and can vary in scale from small projects of one to a few turbines to large, multi-turbine projects (denoted as *utility-scale* or *wind farms*). Utility-scale projects can consist of up to hundreds of wind

turbines. These turbines are normally operated by independent power producers who sell the generated power to the local utility provider [12]. Wind turbine operation and maintenance (O and M) costs, which are known to be the predominant costs that contribute to the cost of wind energy, are generally attributed to a limited number of components, including insurance, land usage, maintenance, repair, spare parts, and administration [8, 13]. For most wind turbines, maintenance and repair account for the largest share of O and M costs. These costs include the following:

- *Downtime*: The revenue lost from turbine downtime is factored into the overall cost of repair. Downtime includes the logistics time for organizing a repair crew and supplies, as well as travel time and the actual time needed to repair the affected component.
- *Labor Costs*: The cost of a service crew is factored into O and M.
- *Crane*: If major repairs or component replacements are necessary, a crane may be needed. The cost of transporting a crane (normally to a remote location) and operating it contributes significantly to O and M.
- *Materials and Consumables*: The magnitude of this cost may vary significantly depending on the component which has failed and the extent of the damage.

It must be noted that O and M costs in offshore wind turbines tend to be significantly higher than that of comparable land-based turbines because they are more difficult to access. Less frequent access for maintenance and repair can lead to large reductions in downtime costs.

18.3 Wind Turbine Theory and Designs

The term wind turbine power systems (WTPS) denotes systems that extract kinetic energy from wind and convert it into usable electrical energy. Along these lines, the size and mechanical complexity of wind turbines can range from relatively small (e.g., household wind turbines) to large, offshore wind turbines. Regardless of the size, all wind turbines incorporate airfoil blades that are pitched into and pushed by the wind, causing rotational power that is ultimately transferred to a generator.

18.3.1 Wind Energy Considerations

In the design process, a number of items about wind power must be considered, including the following:

- *Transient Wind Speed*: Wind speed can change significantly over a relatively short time; thus turbines must be able to adapt to rapidly changing loads. Turbines must also be able to protect from over speed when wind speeds are beyond operating limits.

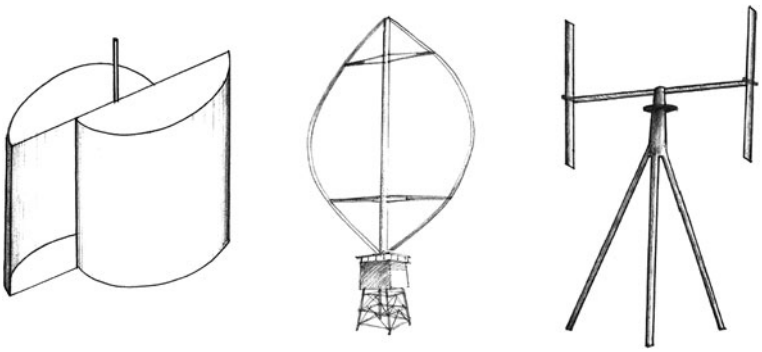

Fig. 18.3 Savonius, Darrieus (eggbeater version), and H-bar VAWTs, from [14]

- *Transient Wind Direction*: Because wind gusts can change direction quickly, wind turbines must be able to adapt to changing directions in order to function effectively.
- *Wind Shear*: Wind shear results in lower wind speeds near the ground, and larger wind speeds with increasing altitude. As a result, rotor blades transmit cyclic loads to the drivetrain.
- *Environmental Conditions*: Wind can contain dirt, dust, and water, which can accelerate damage to critical components within the turbine.
- *Environmental Temperature*: Ambient temperature can influence the viscosity of lubricating oil, which will in turn impact the operation of the entire system.

18.3.2 Wind Turbine Design and Performance

Wind turbines are generally classified into two categories: horizontal-axis wind turbines (HAWTs) and vertical-axis wind turbines (VAWTs). VAWTs incorporate a vertically oriented rotor shaft, with drivetrain components located at their base. Early VAWT designs include Savonius, Darrieus, and Giromill, or H-bar designs (Fig. 18.3). Although VAWTs have shown to have advantages over HAWTs in that they are omnidirectional and their drivetrain components easily maintained, their installation heights are limited, and their blades are prone to cyclic fatigue. Because VAWTs are relatively uncommon among modern turbine designs, they will not be discussed in this manuscript.

HAWTs incorporate drivetrains that are oriented horizontally, in a direction parallel to that of the wind. HAWTs are far more common for utility-scale applications (e.g., greater than 100 kW in capacity) than VAWTs in part due to their capability of being installed at higher altitudes, and consequently,

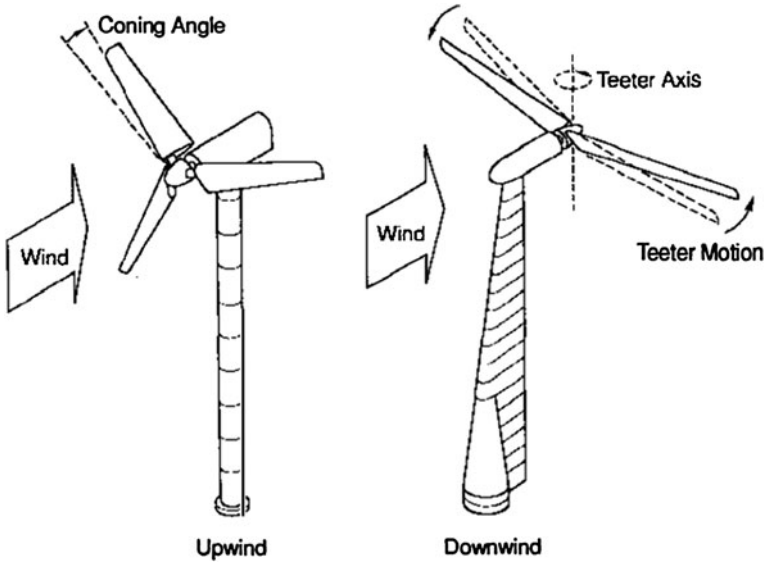

Fig. 18.4 Schematic of upwind, three-bladed HAWT, and downwind, two-bladed HAWT, from [15]

their potential to be exposed to greater wind speeds. The drivetrain components, generator, and associated systems are installed in a nacelle enclosure at the top of a tower, with the nacelle itself angled (yawed) to keep the rotor blades in the direction of the wind. Early wind turbines were designed to position the blades downstream of the support tower and be yawed passively by the wind itself (known as *downwind HAWTs*, shown in Fig. 18.4). However, the blades in downstream HAWTs are exposed to the turbulent wake that is caused by the tower, which was shown to cause fatigue failures due to cyclic loading. For this reason, almost all downwind HAWT designs have been replaced in favor of turbines that position the blades upwind of the tower (i.e., *upwind HAWTs*), as enabled by a yaw system that is actively controlled using a wind sensor and control mechanism. Because upwind HAWT designs are used almost exclusively in modern turbines, they will be the focus of this manuscript.

The power output from a wind turbine is given by the following:

$$P = \frac{1}{2} C_P \rho A U^3 \tag{18.1}$$

where ρ is the density of air, C_P is the power coefficient, A is the rotor swept area (i.e., the area of the imaginary circle formed by the blade tips), and U is the wind speed. The power coefficient C_P, which denotes the fraction of wind power that can converted into usable mechanical work, is primarily a function of the tip speed ratio (commonly denoted as λ), which is defined as the ratio of the rotor tip speed

to free wind speed. The maximum theoretical power coefficient is denoted as the Betz limit, which is specified to be 0.593. In practice, lower maximum power coefficients in the range of 0.47 and below are commonly seen in utility-scale turbines, with optimal tip speed ratios between 6 and 8.

The power coefficient of a wind turbine is also dependent on the blade pitch angle, that is, the angle of attack of the blades with respect to the direction of the wind. Most modern utility-scale turbine designs use pitch angle to control the rotation of the rotor, and in doing so, fall under three main classes: (1) passive stall-controlled, (2) active stall-controlled, and (3) pitch-controlled. Passive stall control indicates that the rotor blades are designed to stall at large wind speeds, and thus do not incorporate a pitching mechanism at the blade roots.

In regard to the solidity of the rotor swept area (i.e., the total blade area divided by the swept area), it is well accepted that utility-scale turbines have three rotor blades, which corresponds to a solidity of approximately 0.0345. Having a high solidity (i.e., more than three rotor blades) results in a relatively narrow range of tip speed ratios λ at which C_P is optimum, in addition to increased production costs due to the large number of blades that must be manufactured, shipped, and installed. Meanwhile, turbines with relatively low solidity (i.e., one or two rotor blades) have been shown to experience excessive cyclic loading within their drivetrain components, and have also been shown to have less aesthetic appeal than 3-bladed turbines. For this reason, almost all utility-scale turbines have three rotor blades.

The rotor speed of the wind turbine must be limited for a number of reasons:

- The tip speed ratio has a narrow range (generally, between 6 and 8) for optimal performance, and it is prudent to maintain the rotor speed within the range for efficiency purposes.
- Extreme rotor tip speeds have been shown to cause excessive noise, because the noise emissions from rotor tips vary by the fifth power of blade speed [16]. For this reason, wind turbine designers are forced to have firmer restrictions on turbine rotational speed when the wind speed, and corresponding ambient noise levels, are relatively low. This limitation is less stringent in the case of offshore wind turbines.
- The rotor and hub must be kept within centrifugal force limits. Since centrifugal force increases with the square of rotation speed, excessive rotation speed can result in catastrophic damage to the rotor and/or bearings.

Based on Eq. 18.1, it can be easily seen that the power rating of a wind turbine is largely dependent on wind speed and rotor swept area. A wind turbine manufacturer can therefore design for increased turbine power capacity by either designing the turbine with longer rotors, or by installing the wind turbine at a location with higher wind speeds. Many wind turbine developers are thus working to install larger turbines offshore, as wind speeds tend to be larger offshore, while visual appearance is less of an issue for large, offshore wind turbines. It must be noted, however, that tip speed limitations require an increase in rotor size to be accompanied by a decrease in rotation speed.

18.3.3 Generator Requirements

The generator within the wind turbine receives rotational energy from the drive-train and converts it into electrical energy. In utility-scale turbines, utility requirements call for wind turbines to produce three-phase alternating current (AC) at a fixed frequency of 60 Hz in the United States or 50 Hz in Europe for transfer to the electrical grid. Two types of generators are common in modern turbines, namely, synchronous generators and asynchronous (otherwise known as induction) generators. Both types of generators operate by spinning a rotor within a stator, with a narrow gap, known as the air gap, separating the two. Because power is generated based upon the movement of an electromagnetic field past the windings within the stator, the frequency of the power that is generated is a function of the rotor speed.

An important parameter pertaining to generator operation is known as the synchronous speed n_s, given as follows:

$$n_s = \frac{60\,f}{p_P} \tag{18.2}$$

where f is the frequency of the generated AC power in Hz and p_p is the number of pole pairs within the generator. The number of pole pairs p_p is normally two, which means that if a generator is to be directly connected to the grid, it would be required to spin at a synchronous speed of $n_s = 1{,}500$ rpm (for a 50 Hz electric grid) or 1,800 rpm (for a 60 Hz grid) in order to match the frequency of generated power with that of the grid. An asynchronous generator, also known as an induction generator, operates near the synchronous speed n_s of 1,500 or 1,800 rpm that corresponds to the local grid frequency. Instead of operating directly at the synchronous speed, asynchronous generators are allowed some amount of slip, s, given as:

$$s = \frac{n_s - n_r}{n_s} \tag{18.3}$$

where n_r is the speed of the rotor. Because an increasingly negative slip causes increased generator torque while any positive slip causes the generator to behave like a motor, it is desirable to limit the magnitude of allowable slip such that the rotor speed is uniform within a tolerance of 1%. Wind turbines with asynchronous generators and direct grid connection must then operate within a relatively narrow speed range, such that they are referred to as *fixed-speed* wind turbines. Fixed-speed wind turbines often have two fixed speeds, as enabled by incorporating either two generators with different ratings and pole pairs or a single generator with two sets of windings [17]. The fixed speed system was the design used by Danish manufacturers between the 1980s and 1990s [18], and is thus considered to be the "traditional" layout. A standard squirrel-cage induction generator, which has stator windings connected to the load/excitation source and rotor windings consisting of electrically connected bars of conducting metal surrounding a soft

iron core, has been the most popular choice for electrical power conversion. Because the rotor speed is relatively low (20 rpm), a multi-stage, speed-increasing gearbox is required with fixed-speed systems.

Since the late 1990s, many wind turbine manufacturers started placing increasing focus on *variable-speed* wind turbines, wherein the operating speed of the rotor and generator varies with wind speed. There are a number of advantages in using variable-speed wind turbine systems, in particular the possibilities to reduce stresses of the mechanical structure, to reduce noise, and to provide better control over the generator power [19, 20]. Variable-speed turbines typically incorporate a multi-stage gearbox and a doubly fed induction generator (DFIG). The DFIG contains windings within both the rotor and stator sections. The power that is generated within the stator is directly connected to the grid, while the induced power from the rotor windings is routed through a frequency converter to the electrical grid. Because only the power from the rotor assembly is fed through the frequency converter, the converter is typically rated as a percentage (approximately 30%) of the full generator power. It must be noted that DFIGs require a slip ring assembly to transfer power between the rotor windings and the stationary electronic components. Because the slip ring wears over time, it requires periodic maintenance and is a source of added cost [21].

Most recently, manufacturers have developed variable-speed wind turbines that incorporate synchronous, low-speed generators with no gearbox—these are known as *direct-drive* wind turbines. The generator produces variable frequency output that is proportional to the rotor speed. However, the output power from the low-speed generator is routed through a full-power frequency converter that changes the generator output power frequency to the 50 or 60 Hz that is required by the grid. Although it can be argued that direct-drive turbines improve reliability and lower cost by removing the gearbox, studies [22] have shown that the increased size, weight, and cost of a low-speed generator and full power converter (as compared to a partial converter) oftentimes compensates for the loss of the gearbox.

18.3.4 Transient Loading

It must also be noted that wind turbines, unlike other forms of electricity production, are designed to generate under a spectrum of power levels [5], and thus must contend with transient loads within their drivetrains. A commonly used means to estimate the power-producing ability and drivetrain loads is to assume that it operates under a certain wind speed distribution. The distributions that are frequently used are Weibull (Fig. 18.5) and Rayleigh distributions [23, 24]. To determine the number of cycles of a drivetrain component at a given load, it is important to determine the total number of hours per year for a particular wind speed. This is done by finding the probability of a particular wind speed for the desired distribution and multiplying it by the number of hours per year. The probability that the wind lies between two wind speeds is given by

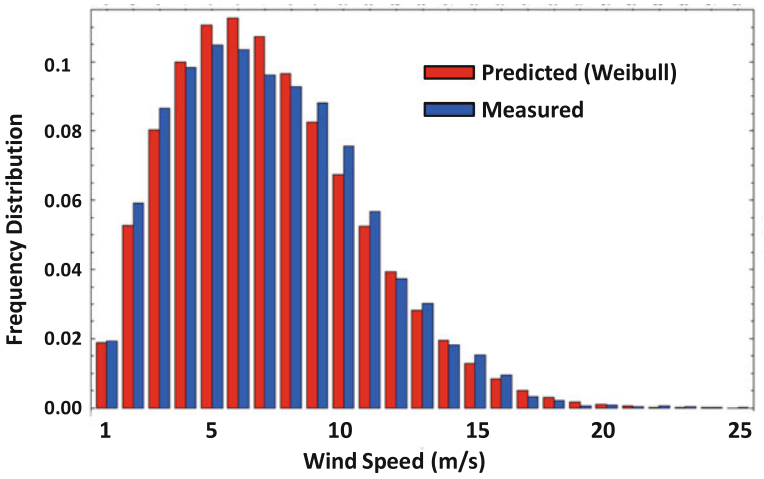

Fig. 18.5 Histogram of predicted and observed wind speeds, from [25]

$$\Pr(u + \Delta u) - \Pr(u - \Delta u) = p(u)\Delta u \tag{18.4}$$

where Pr is the probability function, and $p(u)$ is the probability density function. For the Rayleigh distribution, the probability density function is given by

$$p(u) = \frac{\pi u}{2u_a} \exp\left[-\frac{\pi}{4}\left(\frac{u}{u_a}\right)^2\right] \tag{18.5}$$

where u_a is the average wind velocity. From this, the number of hours that a wind turbine is operated at a given speed is estimated as

$$H(u) = 8760 p(u)\Delta u \tag{18.6}$$

where 8760 represents the total number of hours in a 365-day year [24]. From this analysis, designers can implement a damage criteria such as Palmgren–Miner's rule (as discussed in Sect. 18.5.2.4) to estimate the fatigue lives of components such as gears and bearings.

18.3.5 Power Control

Ideally, a wind turbine should be able to extract as much power as possible up to the rated power of the generator, then limit the extracted power to the rated level as the wind speed increases further. Modern wind turbines are able to maintain the desired amount of power, in part, by controlling the pitch of the rotor blades. Rotor pitch control can take place using one of the following methods:

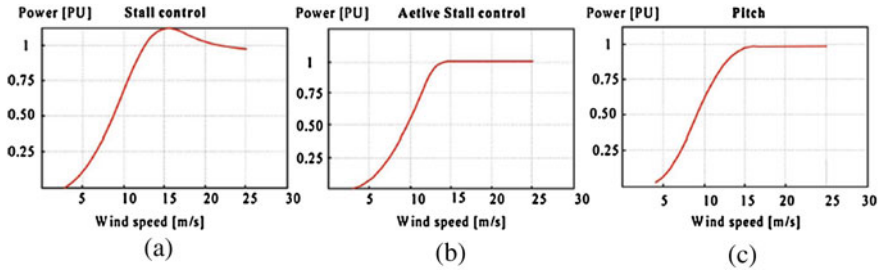

Fig. 18.6 Power characteristics of fixed-speed wind turbines under **a** stall control, **b** active stall control, and **c** pitch control, from [26]

- *Pitch-controlled*: A controller adjusts the rotor blade positions along their long axes to change their angle of attack with the wind [5]. The pitch rotation is enabled by bearings mounted in the hub of the nacelle, with the pitching mechanism activated using either hydraulic or electric stepper motor operation.
- *Passive stall-controlled*: The rotor blades are rigidly attached to the hub at a fixed angle. However, the geometry of the rotor blades are designed aerodynamically to ensure that the blades will stall (i.e., lose lift) when the wind speed exceeds a designated value. This feature serves to protect the turbine from overspeed.
- *Active stall-controlled*: The rotor blades are allowed to rotate along their long axes using a mechanism similar to that of the pitch-controlled system. In active stall-controlled systems however, the controller is programmed slightly differently such that the blades are pitched to stall when wind gusts are excessive.

Each method produces a slightly different power curve (i.e., extracted power vs. wind speed), as shown in Fig. 18.6. The generator torque is also actively controlled to maintain an optimum rotor speed, although this control mechanism can cause undesired load reversals to be transmitted through the gearbox when the wind speed is highly variable.

18.4 Drivetrain Layout

The nacelle of the wind turbine is the external housing that contains the main mechanical components of the system. As shown in Fig. 18.7, these components include the rotor shaft and bearings, a gearbox assembly (if necessary), a lubricant filtration system, a mechanical braking system, a generator, and power electronics. The gearbox transmits power from the main shaft to a high-speed shaft, which, in turn, drives the generator. The drivetrain components and nacelle cover are mounted onto a bedplate, which in turn, is positioned on top of a yaw system that is designed to actively orient the rotor into the wind.

Although a variety of wind turbine drivetrain designs are currently in use, all utility-scale designs generally fall within three main categories [27]. The first

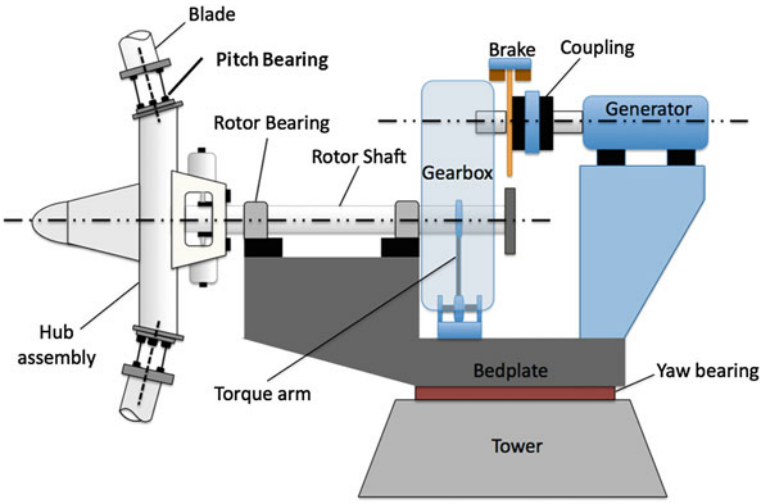

Fig. 18.7 Diagram of components in wind turbine nacelle

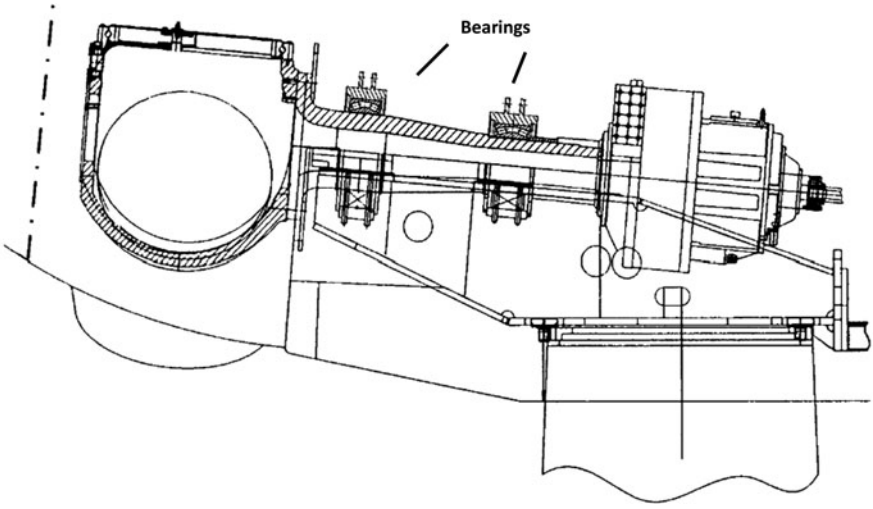

Fig. 18.8 Drivetrain layout featuring two bearings outside the gearbox supporting the main shaft, from [28]

concept (Fig. 18.8) involves the support of the main shaft using two bearings. The bearing nearest the rotor carries both axial and radial loads while the bearing near the gearbox carries radial loads. As a result, the main shaft transfers only torque into the gearbox. Because the gearbox may carry reaction torque towards the bed plate, the gearbox assembly may be fitted with torque arms to transfer the reaction torque to the bedplate. The second concept (Fig. 18.9), known as a

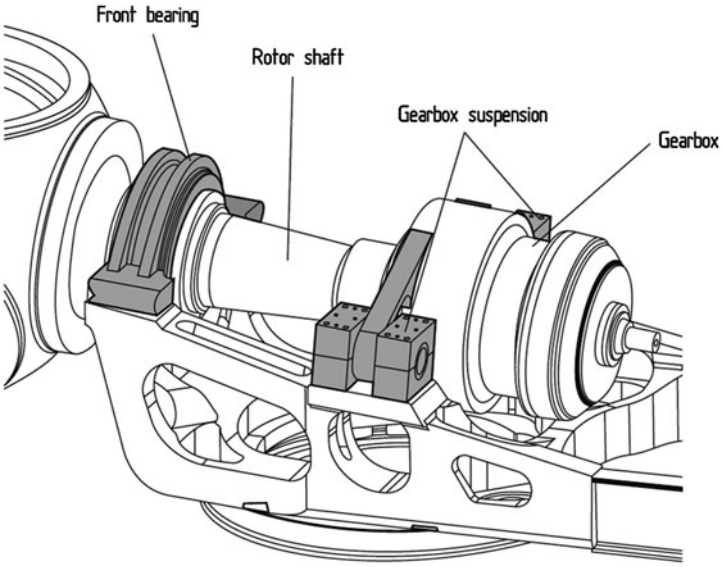

Fig. 18.9 Drivetrain layout incorporating a three-point suspension, with one rotor shaft bearing integrated into the gearbox, from [28]

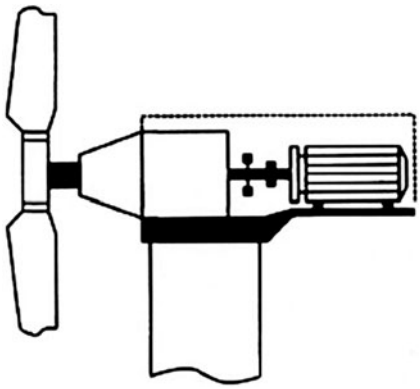

Fig. 18.10 Drivetrain layout with all main bearings integrated in the gearbox, from [27]

"three-point-suspension" design, involves the use of one axial bearing to support the main shaft near the rotor, while a radial bearing supports the opposing end of the shaft from inside the gearbox. The gearbox itself is mounted on the bed plate and is supported by two torque arms. The third category of drivetrain (Fig. 18.10) involves the use of direct integration of the gearbox into the nacelle. In this design, all loads from the rotor enter the gearbox, with all of the rotor support bearings integrated into the gearbox as well. This design can be considered advantageous for the purposes of weight reduction of the nacelle; however, incompatibilities between the gearbox and the remaining components in the nacelle can lead to early failure [27].

18.5 Wind Turbine Tribological Components and Analysis

The tribological components in a wind turbine include rotor support bearings, intermediate gearbox rotor bearings, high-speed bearings, pitch bearings in the hub, epicyclic and parallel gears in the gearbox, a mechanical brake, a roller bearing system in the yaw mechanism, and slip rings in generator (if the generator is a doubly fed induction generator).

18.5.1 Drivetrain Bearings

Rolling-element bearings are incorporated to support the rotor and rotor shaft, the gearbox shafts, and the generator input shaft, with the bearing arrangement depending heavily on the layout of drivetrain. Rotor shaft bearings support the main shaft as well as the rotor blades, operating under dynamic axial and radial loads as well as slow speeds (approximately 20–30 rpm). The rotor blades impose cyclic loads onto the main shaft, thus causing the shaft itself to bend, resulting in misalignment within the bearings. Intermediate-speed and high-speed bearings in the gearbox can also be subject to preliminary damage [29].

It is widely accepted that bearing failure is one of the major issues in wind turbine drivetrain reliability, as the bearings must contend with cyclic and transient loading as well as alignment issues. Studies by Slootweg et al. [30] and Musial et al. [29] relate the start of most drivetrain failures to faulty bearings.

Bearings can be designed to handle purely axial loads, purely radial loads, or a combination of the two. Examples of each type include [31]:

- *Bearings for pure axial load*: Four-point contact ball bearing, spherical roller thrust bearing, tapered roller bearing, and cylindrical roller thrust bearing (Fig. 18.11).
- *Bearings for pure radial load*: Cylindrical roller bearing and toroidal bearing (Fig. 18.12).
- *Bearings for combined axial and radial loads*: Spherical roller bearing, tapered roller bearing, deep-groove ball bearing, angular contact ball bearing (Fig. 18.13).

It must be noted that the locating ability of bearings is designated according to their axial load-handling abilities. A bearing that is capable of supporting axial forces in both directions is known as a *locating* bearing, while a bearing that supports only radial load is designated a *non-locating*, or floating, bearing. Finally, a bearing that supports axial loads in one direction is referred to as a *cross-locating* bearing. Various combinations of bearings can be fitted in a given location to provide complementary load-sharing abilities. For instance, a cylindrical roller bearing can be situated next to a four-point contact ball bearing, such that the bearings in tandem can support both axial and radial loads.

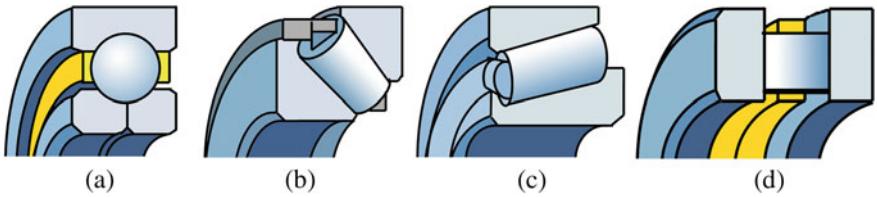

Fig. 18.11 Bearings for purely axial load **a** four-point contact ball bearing, **b** spherical roller thrust bearing, **c** tapered roller bearing, and **d** cylindrical roller thrust bearing [31]

Fig. 18.12 Bearings for purely radial load **a** cylindrical roller bearing, and **b** toroidal bearing [31]

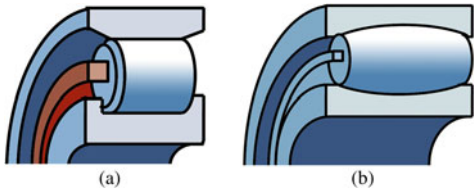

A spherical or tapered roller bearing typically supports the main shaft of most modern wind turbines upwind of the gearbox with rear, non-locating support bearings inside the gearbox [29]. Spherical bearings have the advantage of allowing the bearing's inner and outer ring to be slightly askew with each other without damaging the bearing while running. The spherical bearing has two sets of rollers, allowing support of both radial loads (across the shaft) from the weight of the rotor, shaft, etc. and large axial forces (along the shaft) resulting from wind pressure on the rotor [32]. Thus, the axial load on the main shaft is supported by the main bearing and is not transmitted to the gearbox, which is advantageous for maximizing gearbox reliability.

18.5.1.1 Lubrication Methods

The main shaft bearings are lubricated using either pressure-fed oil lubrication or grease lubrication. The pressure lubrication method uses a circulating oil delivery system that involves the use of pumps, valves, and pipes to supply oil to the bearing. This system is considered to be the most effective because the circulation system regulates the oil temperature while filtering contaminants and metallic wear particles from the oil. However, the complexity of the system and the possibility of lubricant leakage tend to make pressure lubrication impractical for the rotor bearings. For this reason, lubrication with grease is a suitable, low-maintenance alternative which does not require any delivery systems. Grease lubrication is thus used in the rotor bearings of some utility-scale wind turbines [28].

In regard to the bearings in the gearbox (i.e., intermediate-speed, or high-speed bearings), it is well accepted that bearings in the gearbox are generally lubricated using gear oil or some equivalent, which is circulated and distributed using either an oil-splash or circulating oil (i.e., pressure-fed) lubricant delivery system.

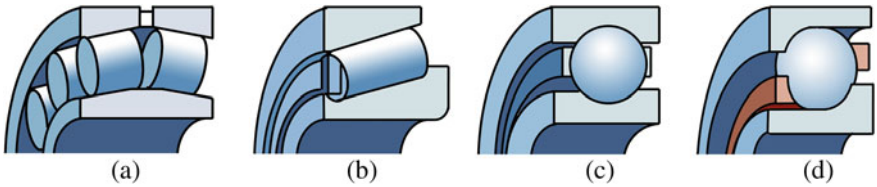

Fig. 18.13 Bearings for combined radial and axial loads **a** spherical roller bearing, **b** tapered roller bearing, **c** deep-groove ball bearing, and **d** angular contact ball bearing [31]

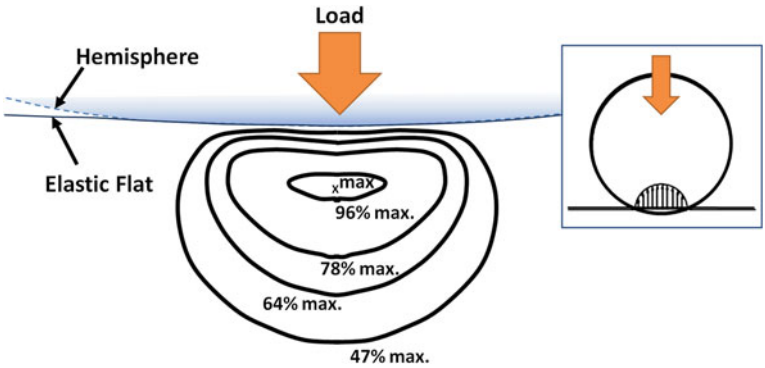

Fig. 18.14 Position of maximum stress for elastic contact between a sphere and a flat, adapted from [34]

18.5.1.2 Bearing Dynamics and Wear

The dynamics of rolling element bearings can be idealized as that of two non-conforming solids which initially touch along a point or a line. Under a compressive load in static conditions, the surfaces deform, causing a contact region of rectangular, ellipsoidal, or spherical shape depending on the geometry of the contacting bodies. Contact of this nature can be analyzed according to Hertzian contact theory [33]. Studies have shown that the contact pressure distribution is maximum in the geometrical center of the contact region, while the maximum shear stress occurs at a defined depth beneath the surface (Fig. 18.14).

As discussed by a report by Kotzalas and Doll [35], there exist a number of failure modes in wind turbine bearings. One of the most common wear modes is rolling contact fatigue, whose occurrence can often be attributed to the relatively large stresses that tend to appear below the surface of rolling elements. These subsurface stresses can produce cracks that form beneath the surface of the rolling elements or raceways, which then propagate to the surface, causing material to be removed from the surface and leaving behind small pits [36] (Fig. 18.15). Fretting wear can also occur within bearings, as wind gusts can cause the bearings to have low-amplitude motion while the system is shut down for maintenance [31].

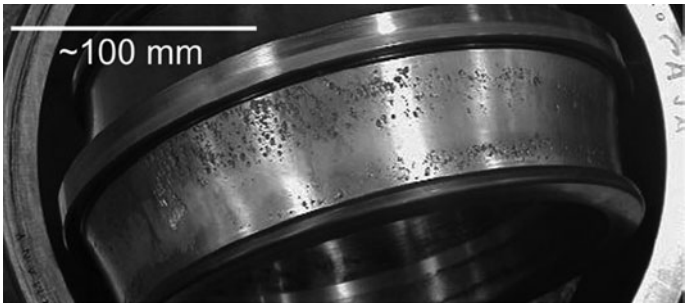

Fig. 18.15 Micropitting in the raceway of a spherical roller bearing, from [39]

Finally, a phenomenon referred to as white-etch area flaking has also been deemed problematic by some groups. Although the detailed physics of this phenomenon is not well understood, recent studies [37, 38] have indicated that this phenomenon can be traced back to the diffusing of hydrogen from the lubricant into the steel, causing the steel to embrittle, and making the raceway surfaces susceptible to flaking wear.

18.5.1.3 Bearing Predictive Modeling

Bearing dynamics and wear are normally predicted using either statistical or numerical methods. The statistical approach involves the use of a fatigue life model (i.e., probability density function) that provides a description of the trend of failure probability, but contains empirical constants that must be filled in using experimental data. The numerical approach, on the other hand, relies on the numerical approaches to determine parameters such as the lubricant hydrodynamic pressure, lubricant film thickness, and bearing and raceway deformation.

Bearing Fatigue Life

The life theory of rolling bearings, as presented by Lundberg and Palmgren [40, 41], is a commonly used method by which the expected lifetimes of rolling bearings are predicted. According to this theory, the rating life of rolling bearings, L_{10}, in millions of revolutions, is given as:

$$L_{10} = \left(\frac{C}{P}\right)^{p} \tag{18.7}$$

where C is the load for which $L_{10} =$ unity, P is the actual bearing load, and p is an exponential constant that has the value of $p = 3$ for ball bearings and $p = 10/3$ for roller bearings. The term L_{10} denotes the number of millions of cycles at which 10% of bearings will begin to fail under the operating conditions given.

Lubricant Film Thickness and Lambda Ratio

Wind turbine bearings are generally lubricated using grease or high-viscosity mineral or synthetic oil to minimize surface contact. Lubrication modes are generally classified according to one of three regimes—boundary lubrication, elastohydrodynamic lubrication (EHL), and full film (i.e., hydrodynamic) lubrication. Bearing interfaces typically operate within the EHL regime due to the large applied loads. Because EHL tends to take place under high loads and/or low sliding speeds, it is characterized by the interplay between the pressure-based elastic deformation of the contacting surfaces and the viscosity and density enhancements of the lubricant [42–45]. The lubricant itself experiences a sudden rise in pressure, from ambient to over 1 GPa, within the interface, causing (under ideal conditions) separation of the solid surfaces and minimizing of surface wear. The study of EHL has been extensively investigated by a number of researchers over the past half-century, as initiated by the pioneering work of Grubin [44, 46], and Dowson and Higginson [47, 48], and collaborators.

Assuming that both surfaces are separated by a thin film of lubricant, EHL theory is governed by equations describing the lubricant pressurization, viscosity, and density enhancement, as well as an elasticity equation that describes the deformation of the gear tooth surfaces under load [49]. Assuming the contact takes place along a line (i.e., spur gear contact without edge effects), the lubricant pressure, p, is governed by the Reynolds Equation:

$$\frac{\partial}{\partial x}\left(\frac{\rho h^3}{\eta}\frac{\partial p}{\partial x}\right) = 6U\frac{\partial(\rho h)}{\partial x} + 12\frac{\partial(\rho h)}{\partial t} \tag{18.8}$$

where ρ and η are the density and viscosity, respectively, of the lubricant, t is time, and U is the sum of the surface velocities. The pressure distribution is typically subjected to zero-pressure inlet and Reynolds outlet boundary conditions. The lubricant film thickness h is given by the following:

$$h = h_0 + g_0 + \delta \tag{18.9}$$

where h_0 is the reference film thickness, g_0 is the undeflected geometric gap between the two surfaces, and δ is the composite elastic deformation of both surfaces. The geometric gap is calculated to be:

$$g_0 = \frac{x^2}{2R_{\text{eq}}} \tag{18.10}$$

where $R_{\text{eq}} = (1/R_A + 1/R_B)^{-1}$ is the equivalent radius of curvature as defined by Hertzian theory. The surface deflection, meanwhile, is governed by the elasticity equation for semi-infinite solids under applied load:

$$\delta(x) = -\frac{1}{\pi E'}\int_{-b}^{a} p(s)\ln|x-s|\mathrm{d}s \tag{18.11}$$

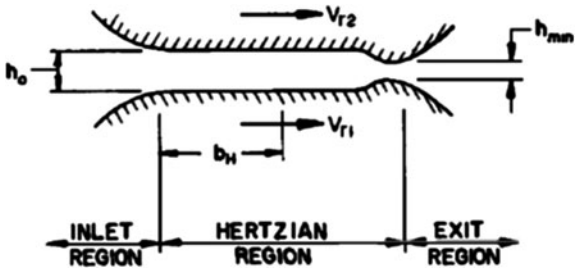

Fig. 18.16 Film thickness distribution in EHL, from [51]

where v is Poisson's ratio and $E' = 2((1 - v_A^2)/E_A + (1 - v_B^2)/E_B)^{-1}$ is the Young's modulus.

The lubricant viscosity, meanwhile, has been shown to increase with increasing pressure. A simplified model that describes this phenomenon, known as piezo-viscosity, is given by the Barus Equation, as follows:

$$\eta = \eta_0 \exp(\alpha p) \tag{18.12}$$

where η_0 is the lubricant viscosity at ambient pressure. The lubricant density, which also increases within the EHL interface, can be modeled by means of a density–pressure relationship presented by Dowson and Higginson [48]:

$$\rho = \rho_0 \frac{(1 + \gamma p)}{(1 + \lambda p)} \tag{18.13}$$

where $\gamma = 2.266 \times 10^{-9}$ Pa^{-1}, $\lambda = 1.683 \times 10^{-9}$ Pa^{-1}, and ρ_0 is the density at ambient pressure.

Equations 18.8–18.13 can be solved simultaneously using iterative or inverse numerical methods [50]. Studies have shown that the film thickness h within the EHL interface is approximately uniform, with the exception of a sudden decrease in h that occurs near the exit of the interface (Fig. 18.16).The lubricant pressure distribution, meanwhile, is found to have a similar parabolic profile as that which would be predicted for Hertzian contact (Fig. 18.17), with the exception of a pressure spike that occurs in the same location as where the film thickness suddenly drops off. Both the pressure and film thickness profiles have been analyzed extensively, and verified experimentally.

The film thickness distribution within EHL is a subject of tremendous interest because the lubricant film is the primary means by which the surface asperities of the gear teeth are separated from one another. The EHL film thickness is generally known to have a relatively flat region followed by a sharp decrease at the lubricant exit. It is thus characterized by two parameters, namely, the central film thickness h_c, and the minimum film thickness $h_{\min}$. If the combined height of the asperities on each mating gear is larger than either the central or minimum film thickness, asperity–asperity contact may occur. Such contact will inevitably lead to surface damage such as abrasive wear, micropitting, scuffing, and crack formation. To characterize the effect of film thickness separation versus asperity–asperity contact,

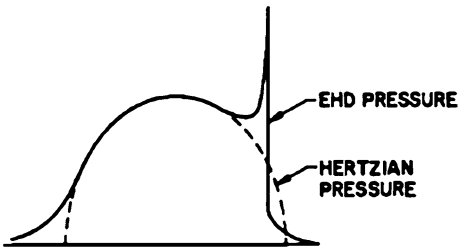

Fig. 18.17 Lubricant pressure distribution in EHL, from [51]

Table 18.1 Wear patterns for various lambda ratios (reproduced from [53])

λ value	Wear pattern
$\lambda < 1$	Surface smearing, deformation, abrasive wear
$1 \leq \lambda < 1.5$	Smoothing of rough areas, spallation
$1.5 \leq \lambda < 3$	Some smoothing of rough areas
$3 \leq \lambda < 4$	Minimal wear
$4 \leq \lambda$	Full separation by EHL film

Tallian [52] introduced a parameter known as lambda ratio λ, known as follows [53]:

$$\lambda = \frac{h_c}{\sqrt{\sigma_1^2 + \sigma_2^2}} \tag{18.14}$$

where σ_1 and σ_2 are the root-mean-square (RMS) roughness of the two contacting surfaces. Studies have shown that the lambda ratio governs the wear pattern, if any, that is experienced by the geartrain, according to Table 18.1.

It can thus be seen to be advantageous to have a lambda ratio that is as large as possible in order to minimize the possibility of gear wear. Recent efforts have thus been taken towards improving the surface finish of gears. Experimental tests by Doll and collaborators [54, 55] have shown that superfinishing (surface polishing to sub-micron roughness) causes noticeable improvement in anti-wear performance.

18.5.2 Gearbox

Utility-scale fixed-speed and variable-speed wind turbines rely upon a gearbox to increase the slow-moving, high-torque input from the rotor to the high-speed output that is required by the generator. The gearing ratio, G, for a wind turbine transmission is defined as follows:

$$G = \frac{n_{\text{generator}}}{n_{\text{rotor}}} \tag{18.15}$$

where $n_{\text{generator}}$ is the rotational speed of the generator and n_{rotor} is the rotational speed of the rotor, both in rpm. A wind turbine that incorporates a generator

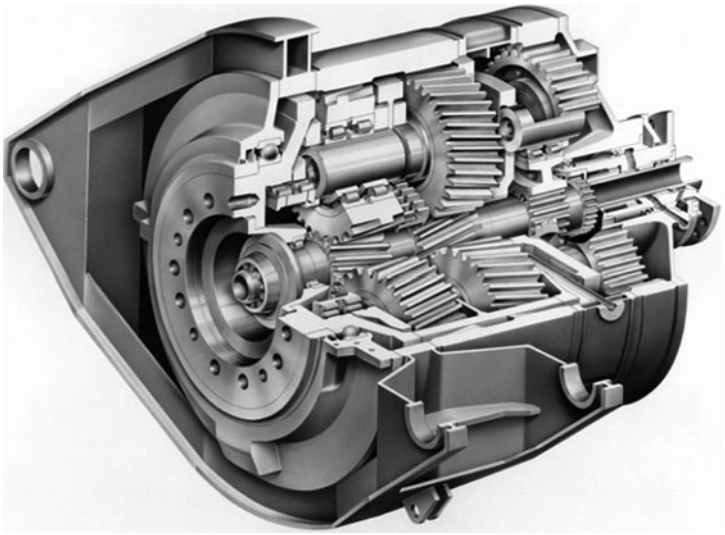

Fig. 18.18 Configuration of three-stage gear for 2–3 MW wind turbine, from [28]

operating at 1,500 rpm and rotor operating at 20 rpm would require a gearbox with gearing ratio of $G = 75$ [56]. The total gearing ratio can be considered a product of the ratio of the individual stages, i.e.,

$$G = G_1 \times G_2 \cdots \times G_N \tag{18.16}$$

where N is the number of stages in the gearbox. Modern turbines generally incorporate at least three gearing stages in the gearbox. One or more stages is generally of a planetary, or epicyclic configuration, while the remaining stages are typically of a parallel (i.e., gears with fixed, parallel axes) configuration (Fig. 18.18). Epicyclic gears incorporate multiple outer gears whose centers revolve around a single, center gear. The revolving gears are denoted as "planets," while the center gear is the "sun". An outer ring gear is located outside the planet gears [56]. For wind applications, the number of planets is normally chosen to be three. Epicyclic gears have seen significant use in wind applications due to the fact that they can transfer a higher torque density than parallel stages, which enables them to be relatively lightweight and compact as compared to parallel gears of similar load capacity. The epicyclic stage is normally designed for gear ratios up to $G_i = 7$, while parallel stages can handle gear ratios up to $G_i = 5$ [27].

Although the electrical systems in wind turbine systems are generally most prone to failure, gearbox and components tend to be the costliest to maintain and replace [10, 57]; thus gearbox reliability is considered a critical issue in wind turbine design and operation. Studies have shown that less-than-desired reliability

in wind turbine gearboxes can be attributed to a number of different factors, including the following:

- Wind gusts and generator connection/disconnection from the electrical grid may cause undesired load reversals in the gearbox, which can lead to excessive contact stresses in the gear flanks [35].
- Undesired movement of the drivetrain, which can be caused by deformations within the bedplate, can cause misalignment of the gearbox with the generator shafts. This misalignment results in unexpected damage to the high-speed bearings, which leads to damage in the high-speed gears [56].
- The gearbox may be subject to particulate contamination, which may lead to surface pitting in the gears.
- Excessively high oil temperatures may result in scuffing wear in the gears [28], thus necessitating the use of oil coolers and filters in the lubricant delivery system.

18.5.2.1 Gear Geometry

The tooth profile of spur and helical gears is based on a truncated involute curve (Fig. 18.19), which is defined as a curve that connects a locus of points that are generated at the end of a taut string when it is unwound from the tangent of a base circle (known as the evolute). Litvin and Fuentes [58] involute gearing, first proposed by Euler, has many advantages in its use, including: (1) ease of manufacturability, (2) lack of transmission errors when the gear center distance is changed, and (3) the tooth-to-tooth force is applied along a constant line of action throughout the time of meshing. Through geometrical analysis, it can be found that the geometry of contacting involute gear teeth can be represented by circular discs of varying radii. For this reason, the contact theory of Hertz [33] has the ability to provide a reasonable solution for the elastic deformation, pressure distribution, and real contact area between mating teeth, although it must be noted that Hertzian analysis is based on the assumption of static, dry (nonlubricated), and frictionless conditions—none of which are experienced between moving gear teeth. A more appropriate analysis involves the combined study of lubricant flow and pressurization along with deflection of tooth surfaces, as will be discussed in Sect. 18.5.1.3.

Both spur and helical gearing geometries are common within wind turbine gearboxes. In the case of spur gears, the contact region is a straight line across the depth of the tooth, such that at any time either one or two teeth are in contact. Helical gears, however, are skewed in the axial direction, causing each tooth to appear as a segment of a helix. Because the teeth are angled with respect to the axis of rotation, the contact region is composed of a series of slanted lines, with several teeth in contact at a given time. The angled teeth engage more gradually than do spur gear teeth, causing them to run more smoothly and quietly [60]. In regard to loading, spur gears impose only radial loads on their bearings.

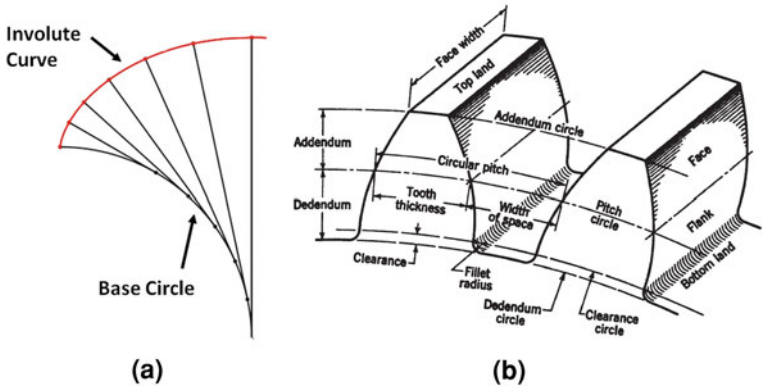

Fig. 18.19 Geometry of involute spur gears **a** involute curve generation, **b** spur gear tooth nomenclature, from [59]

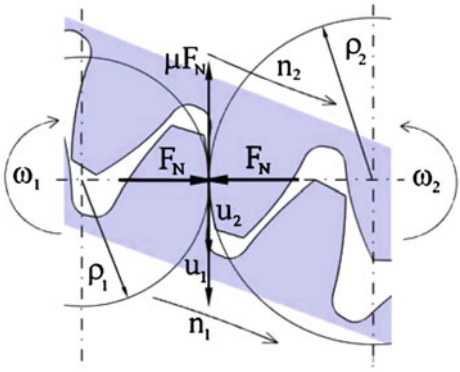

Fig. 18.20 Equivalent radius of curvature for contacting gear teeth, from [62]

Single helical gears, meanwhile, impose both thrust and radial loads on their bearings. Double helical gears, which are side-to-side combinations of helical gears of opposing axial skewness, develop equal and opposite thrust reactions which serve to cancel out the thrust load [61].

18.5.2.2 Gear Loads and EHL Calculations

The geometry of contacting spur gear teeth is likened to that which is formed by the contact of two rotating circular discs of varying radii. The radii of curvature (Fig. 18.20) of the driving gear (denoted as *Gear A*) and the driven gear (denoted as *Gear B*) are given as:

$$R_A = r_A \sin(\psi) + S \tag{18.17a}$$

$$R_B = r_B \sin(\psi) - S \tag{18.17b}$$

where r_A and r_B are the pitch radii of *Gears A* and *B*, respectively, ψ is the contact angle, and S is the distance of the contact point from the pitch point [53].

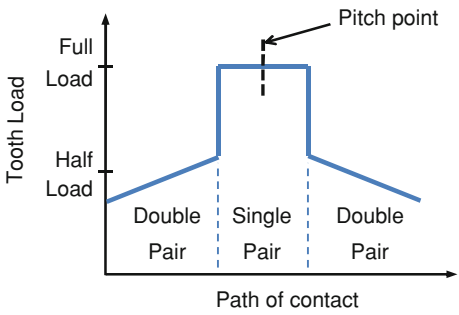

Fig. 18.21 Load sharing of gear tooth during a meshing cycle

The torque that is applied to the gear is given by [63]:

$$T = \frac{P}{\omega} \tag{18.18}$$

where P is the transmitted power, and $\omega = 2\pi N$ is the rotation speed. The normal load that is applied to each meshing tooth is then found as:

$$W_A = s_A\left(\frac{T}{R_A \cos(\psi)}\right) \tag{18.19a}$$

$$W_B = s_B\left(\frac{T}{R_B \cos(\psi)}\right) \tag{18.19b}$$

where s_A and s_B are the percentage of torques shared by the contacting teeth of *Gear A* and *Gear B*, respectively. The load sharing percentages are functions of the contact ratio m_c (a measure of the average number of teeth in contact as a given instant), as well as elastic and surface profile properties of the gear teeth [64]. The torque is shared between contacting teeth based upon their meshing positions, as it is dependent on the elastic stiffness of each tooth at the point of contact (Fig. 18.21). In the case of epicyclic gearing, studies have shown that under ideal conditions, the rotating load is divided evenly by the number of planets, which is further shared by the number of contacting teeth on each planet [65].

Using the loads W_A and W_B and the equivalent radii of curvature R_A and R_B, one can perform EHL analysis to determine the lubricant film thickness and lambda ratio between mating gear teeth in a similar manner as that done for bearings (Sect. 18.5.1.3).

18.5.2.3 Gear Dynamics and Wear

The gears in the transmission experience rolling and sliding contact along the gear tooth faces. Contacting gear teeth slide and roll against one another as they come into mesh and then transition into pure rolling contact at the pitch point. As the teeth move out of mesh, the contact mode transitions back to combined rolling and sliding.

Fig. 18.22 Gear tooth surfaces with scuffing damage, from [67]

In the case of helical gears, it must be noted that an involute helical gear can be analyzed as a set of spur gears with infinitely small width, with each of the spur gears rotated with respect to the adjacent gear to comprise the helical shape [66].

A review by Errichello [51] classifies gear failure according to the categories of overload, bending fatigue, Hertzian fatigue, wear, and scuffing. The primary failure modes in wind turbine gears are generally scuffing, pitting, and abrasive wear, as discussed in the following sections.

Scuffing

This failure mode is caused by rapid adhesion and/or welding of the asperities of contacting gear teeth, followed by the tearing of one or both surfaces as the gears teeth slide past one another (Fig. 18.22). It results in the transfer of material from one tooth surface to another. Scuffing damage can occur if the lubricant film thickness is too low, in which case the oxide layers that normally protect the gear tooth surfaces may be penetrated, and the bare metal surfaces may weld together, resulting in the tearing of the metallic junction.

Although small lubricant film thickness is one condition that is necessary for scuffing to occur, it by itself will not cause scuffing single-handedly. On the contrary, studies have shown that the metallic welding phenomenon that occurs during scuffing is preceded by localized frictional heating, which itself is the result of large contact pressures and elevated sliding velocities between the gear tooth surfaces. The critical temperature theory presented by Blok [68], a widely used criterion for predicting scuffing, predicts that scuffing will occur when the maximum contact temperature exceeds a given value. To minimize the possibility of scuffing, mineral and synthetic lubricants may include anti-scuff, or extreme

pressure (EP), additives, which contain sulfur, phosphorus, or other compounds that create a protective layer on gear surfaces [31].

Pitting

This failure mode, considered to be a Hertzian failure mode, is characterized by the formation of surface or subsurface cracks, which propagate to the surface, causing small pits to remain in the surface. The formation of micron-scale pits is known as micropitting. It must be noted that when a micropitted surface is subjected to subsequent loading cycles, several micropits may grow together, leaving behind a larger pit known as a macropit. The formation of macropits generally leads to vibration and transmission error within the gearbox, as well as overall tooth failure [69]. The probability of micropitting can be reduced by keeping the lubricant film thickness (i.e., lambda ratio) high, as damage can most readily occur on gear teeth with rough surfaces or with an insufficient lubricant film. Surface treatment techniques such as carburizing and superfinishing [70] have promise for increasing pitting resistance, although the cost of these procedures may be of concern.

Abrasive Wear

This failure mode is generally caused by hard contaminant particles that entrain into the interface. Particles that are introduced between sliding interfaces abrade material off each surface creating indentations. These indents create high local stresses and are the primary cause for surface-related fatigue failures [71]. Contaminant particles can be created during the manufacturing, assembly, or run-in processes, be ingested from the environment through breathers or seals, or be internally generated. Further details on particulate contamination in wind turbine drivetrains are given in Sect. 18.6.2.

Bending Fatigue

In addition to lubricant film thickness, an important consideration in geartrain operation involves the bending strength of the gear teeth. If the bending stress extends beyond design criteria, cracks may initiate at the base of the tooth and propagate through its base, causing it to break away from the base of the gear wheel [72]. Most gears, particularly, high contact ratio spur gears, may continue to transmit load after a tooth failure. However, the loss of a gear tooth may cause increased levels of noise and vibration that may lead to subsequent damage to the bearings or other areas of the gearbox [73].

The well-known Lewis equation [59, 74], presented by Wilfred Lewis in 1892, is a classical method to estimate the bending stress in spur gear teeth. According to the Lewis equation, the bending stress σ at the tooth root is given by the following:

$$\sigma = \frac{W}{pBy}$$

where W is the transmitted load, p is the circular pitch, B is the width of the tooth face, and y is a dimensionless form factor which depends on the shape of the tooth. More recently, workers such as Dolan and Broghamer [75] and Kelley and Pedersen [76] have developed more sophisticated formulas for gear tooth bending stress based upon photoelastic experimental measurements. More recent studies have employed FEA to enable an accurate prediction of bending stresses [77, 78].

18.5.2.4 Fatigue Life Prediction

The Palmgren–Miner Linear Cumulative Fatigue Damage Theory (Miner's Rule) is used to calculate the resultant pitting or bending fatigue lives for gears that are subjected to highly varying loads [79, 80]. According to Miner's Rule, failure occurs when:

$$\frac{n_1}{N_1} + \frac{n_2}{N_2} + \cdots + \frac{n_i}{N_i} = 1$$

where n_i is the number of cycles at the ith stress level, N_i is the number of cycles to failure corresponding to the ith stress level, and n_i/N_i is the damage ratio at the ith stress level. It must be noted that a significant limitation in the Palmgren–Miner theory is that the loading sequence (i.e., the order of applied loads) is not considered.

18.5.2.5 Power Loss and Noise

Modern gearboxes produce relatively small power losses, with the main sources of power loss being attributed to tooth-flank friction. As a rule of thumb, parallel gear losses are assumed to be 2% of the full load per stage, while planetary gear losses are assumed to be 1% per stage. The frictional losses result in heat generation and noise emission [22]. Although the generated noise from the gearbox constitutes only a small fraction of the power loss, it can still be noticeable to the point where it can draw complaints from nearby residents (in the case of land-based turbines). To minimize noise, gearbox manufacturers must ensure smooth gear meshing by using high-quality design and manufacturing techniques [28]. The nacelle fairing is also acoustically insulated to prevent sound transmission into the air.

18.5.3 Pitch and Yaw Bearings

Blade pitching systems are used to control power and rotor speed, while yaw systems are used to orient the rotor perpendicular to the wind direction.

The bearings that are used for pitch and yaw systems are often discussed within a similar context, as their ranges of motion and wear modes are often similar to one another. Additionally, both pitch and yaw bearings experience similar types of loading—namely, an eccentrically applied thrust, which can be divided into a pure axial load and an overturning moment load [81]. As a result, the fatigue lives of both pitch and yaw bearings can be estimated using a single life rating predictive approach. It is expected that the static loads that are applied to pitch and yaw bearings will cause some degree of permanent deformation in the raceways and rolling elements; however, experience has shown that a deformation of 1/10,000th of the rolling element diameter is tolerable for successful operation.

18.5.3.1 Pitch Bearing

Blade pitching systems, which actively rotate blades along their longitudinal axes, are used in active-pitch and active-stall controlled wind turbine systems. The pitching motion is typically driven by hydraulic actuators [82] or electric motors. The pitch control system is critical for utility-scale turbines, as it allows the system to optimize power extraction and minimize unnecessary loads. Above all else, the pitching system is employed as a fail-safe aerodynamic brake to stop the turbine when wind speeds become excessive [28], thus making the pitching system critical for preventing catastrophic failure of the whole turbine [8]. While a pitching range of 20–25° is generally sufficient for controlling the power and speed of the rotor, aerodynamic braking necessitates that the blades have the ability to be placed into the *feathered* position (i.e., parallel to oncoming airflow), which minimizes lift, causing the turbine to brake.

The use of a pitching system necessitates that the blades be exclusively supported by rolling element bearings at their roots. The bearings themselves are subject to large static loads as well as centrifugal and cyclic bending loads when the turbine is in operation. Most modern turbines use four-point contact bearings or ball bearing slewing rings for pitch operation. Turbines with smaller rotor blades can suffice with a single-row arrangement in their pitch bearings, while larger rotor blades require double-row four-point bearings.

Pitch bearings are generally lubricated using grease with a high-viscosity base oil. Similar to drivetrain bearings, the grease in pitch bearings should maintain the thickest lubricant film possible to prevent premature damage. Because pitch bearings operate under slight oscillatory motion, fretting wear and/or false brinnelling can occur when the lubricant film is insufficient. Additionally, a report by the National Renewable Energy Laboratory (NREL) suggested the pitch bearing be periodically (i.e., once per day) rotated through a large-amplitude oscillation cycle in order to redistribute grease that has been previously displaced [81].

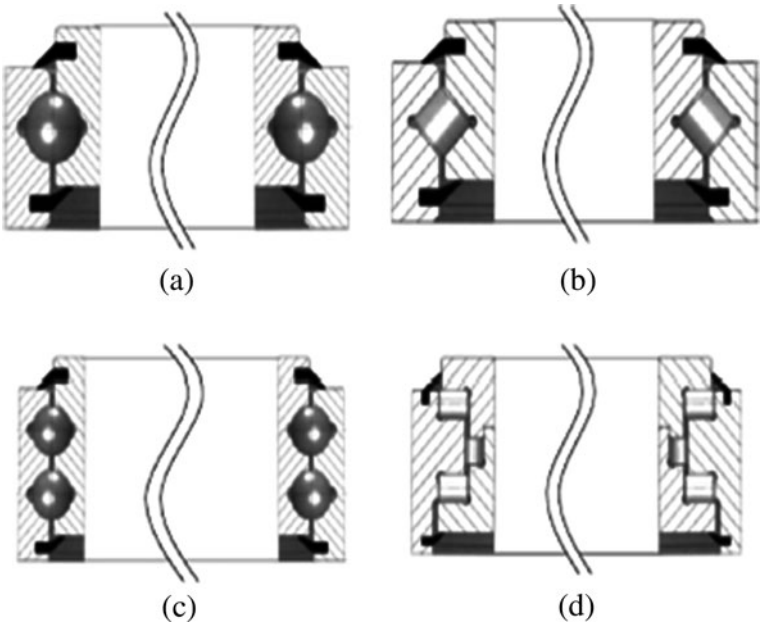

Fig. 18.23 Different types of slewing bearings **a** four-contact-point single row ball bearing, **b** crossed cylindrical roller bearing, **c** four-contact-point-double row ball bearing, and **d** three-row cylindrical roller bearing, from [83]

18.5.3.2 Yaw Bearing

The yaw mechanism rotates the nacelle about its vertical axis to keep the rotors oriented into the wind. Ideally, yaw bearings should provide smooth rotation and long service life as well as yaw damping to prevent unwanted yaw oscillations. Most turbines thus employ roller bearings or ball bearings in their yaw drives, although recent interest has been directed towards gliding bearings that use low-friction synthetic sliding elements in place of balls or rollers. Ball bearing configurations are often single-row, four-point contact ball bearings, although double-row, eight-point contact ball bearings are also used (Fig. 18.23). Double-row bearings have been shown to have the advantage of lower Hertzian stresses and increased fatigue life; however, the double-row arrangement incurs higher manufacturing costs than that of single-row bearings [81].

Similar to pitch drives, yaw drives can be equipped with either hydraulic or electric motors, although electric motors are most popular with modern, large turbines. Usually, the yaw bearings are driven using one or more electric motors in the nacelle, so the bearings contain gears in the inner or outer ring. The yawing motion is usually done only a few degrees at a time [84]. Once the nacelle is in the desired orientation, two or more yaw brakes are typically applied, acting on a brake ring located either inside the tower or the nacelle. The yaw brakes provide

stabilization of the nacelle under varying wind loads, while also preventing the yaw drive from absorbing the yawing moment.

18.5.3.3 Fatigue Life Prediction for Pitch and Yaw Bearings

Because pitch and yaw bearings exhibit oscillatory motion and do not spin continuously, the life estimation theory of Lundberg and Palmgren (Eq. 18.7), which predicts lifetime in terms of number of rolling cycles to probable failure, is not directly applicable. However, studies have shown that the Lundberg–almgren estimation can be modified to apply to oscillating bearings based upon the critical angle of oscillation θ_{crit}, which is calculated as:

$$\theta_{\text{crit}} = \begin{cases} \dfrac{720^\circ}{Z(1-\gamma)} & \text{(outer raceway)} \\ \dfrac{720^\circ}{Z(1+\gamma)} & \text{(inner raceway)} \end{cases} \tag{18.20}$$

where Z is the total number of rolling elements (whether loaded or unloaded) and γ is the contact angle. If the oscillation angle (denoted as θ) is less than θ_{crit}, each rolling element has its own discrete stressed volume within the raceway and the modified axial load rating is given by:

$$C_{a,\text{osc}} = \begin{cases} C_a \left(\dfrac{180^\circ}{\theta}\right)^{3/10} Z^{0.033} & \text{(ball bearings)} \\ C_a \left(\dfrac{180^\circ}{\theta}\right)^{2/9} Z^{0.028} & \text{(roller bearings)} \end{cases} \tag{18.21}$$

where C_a is the actual axial load. However, if θ is greater than θ_{crit}, the contact stresses of the individual rolling elements overlap, and the modified axial load rating is given by:

$$C_{a,\text{osc}} = C_a \left(\frac{180^\circ}{\theta}\right)^{1/p} \tag{18.22}$$

where $p = 3$ for ball bearings and $p = 4$ for roller bearings. If the speed of pitch and yaw bearings is denoted in terms of oscillations per minute, the fatigue life, expressed in terms of millions of oscillations, is calculated as [36, 81]:

$$L_{10} = \left(\frac{C_{a,\text{osc}}}{P_{\text{ea}}}\right)^3 \text{for thrust ball bearings, or} \tag{18.23a}$$

$$L_{10} = \left(\frac{C_{a,\text{osc}}}{P_{\text{ea}}}\right)^{10/3} \text{for thrust roller bearings,} \tag{18.23b)}$$

where P_{ea} is the dynamic equivalent axial load.

18.5.4 Mechanical Brake

Modern wind turbines incorporate a mechanical brake on the high-speed section of the drivetrain, normally between the gearbox and the generator. This mechanical brake, which almost always is in the form of a disk brake, is primarily responsible for locking down the rotor during shutdown such that servicing and repair work can take place. Beyond functioning as a parking brake, some turbines employ the mechanical brake as a secondary braking system to complement aerodynamic braking during operation. On larger wind turbines, the mechanical brake is situated on the high-speed side of the gearbox to minimize the size and weight of the brake disk. Because of its position on the high-speed shaft, the use of the mechanical brake can be detrimental towards gearbox reliability. At standstill, braking loads oftentimes contend with forces from wind turbulence, causing small oscillatory movements of the gear teeth. These motions can result in fretting wear in the gear teeth [28].

18.6 Contamination Effects

Gear oil recirculates through wind turbine gearboxes, lubricating mating surfaces and removing heat. Unfortunately, contaminant particles suspended in the gear oil, as well as water in the parts per million (ppm) range, can significantly degrade the performance and reliability of gearboxes.

Sources of contaminant particles include: cutting and grinding swarf built-in from manufacturing, ingression of airborne abrasives through vents and mechanical seals, and internally generated wear debris and metal oxide corrosion products. To quantify particulate contamination levels, the International Organization for Standardization (ISO) created cleanliness codes that serve as a universal standard for measuring and reporting contamination levels in fluids. Based upon a milliliter sample of lubricant, ISO codes are defined according to the nomenclature $\alpha/\beta/\gamma$, where α, β, and γ denote the number of particles greater than 4, 6, and 14 μm in size, respectively, per milliliter of lubricant. It can be easily seen that the lower the code, the cleaner the lubricant, and thus the aim for wind turbine filtration and monitoring is to keep the code as low as possible. In modern turbines, well-filtered gearbox lubricants may have a code of 16/14/11 or below.

In addition to particulate contaminants, small amounts of water dissolve in lubricating oils and hydraulic fluids. The maximum amount of dissolved water (the saturation level) is typically 300–500 ppm, depending on base stock and additives. Water contamination in excess of the saturation level is termed *free water*, which settles to low points of the system. Emulsified free water—droplets on the order of 1 μm—remains suspended in the oil and gives it a hazy to milky appearance depending on the amount present. Sources of water include humidity ingressing

Table 18.2 Hard particle contamination problems in wind turbine gearboxes

Problem	Summary
Surface-initiated fatigue spalling	3-body wear in rolling contacts. Hard ductile particles dent surfaces, followed by crack propagation leading to fatigue spalling, a.k.a. pitting, cratering of surfaces
Abrasive wear	3-body wear in sliding contacts. Hard particles plough through and cut away surface material, leading to loss of clearance and rough surfaces accompanied by high friction
Accelerated oil oxidation	Catalytic surfaces of fresh metal wear debris accelerate oil oxidation, lead to acidity, oil thickening, and sticky fouling deposits

Table 18.3 Water contamination problems in wind turbine gearboxes

Problem	Summary
Corrosion	Due to free water, especially if acids present from oil degradation and/or microbial growth. Ion currents in aqueous solution. Leads to pitting, leakage, and breakage
Foaming	Due to free water. Leads to air blockage within the oil distribution system, and spillage
Loss of oil film	Due to free water. Water in contact zone cannot support load, allowing opposing surfaces to contact. Results in adhesive wear, high friction, and seizure
Additive drop-out	Due to free and dissolved water. Depletion of hydrophilic additives. Also breaking colloidal suspensions of additives. Leads to loss of additives and fouling of parts
Microbial growth	Due to free water. Colonization of oil by bacteria and/or fungi. Results in: acids, fouling slimes; health issues
Surface-initiated Fatigue spalling	Due to dissolved water carried by gear oil to the tips of propagating cracks. Surfaces of fresh cracks are highly reactive, dissociating water molecules into O_2 and H_2. H_2 migrates into and weakens steel by hydrogen embrittlement. Cracks spread faster, reducing life of rolling elements and resulting in fatigue spalling, pits, and craters
Accelerated oil oxidation	Due to dissolved water, especially if metal wear debris present. Increases rate of oil oxidation by up to 2 orders of magnitude. Leads to acidity, oil thickening, fouling deposits
Hydrolysis	Due to dissolved water. Decomposition of ester-based additives. Leads to loss of additives, formation of acids, and sometime fouling gels

through vents and mechanical seals as well as liquid water incurred during transportation and storage.

18.6.1 Contamination-Based Tribological Problems

Problems caused by particle and water contamination in wind turbine gearboxes are listed in Tables 18.2 and 18.3. Synopses of these problems are provided in the following sections.

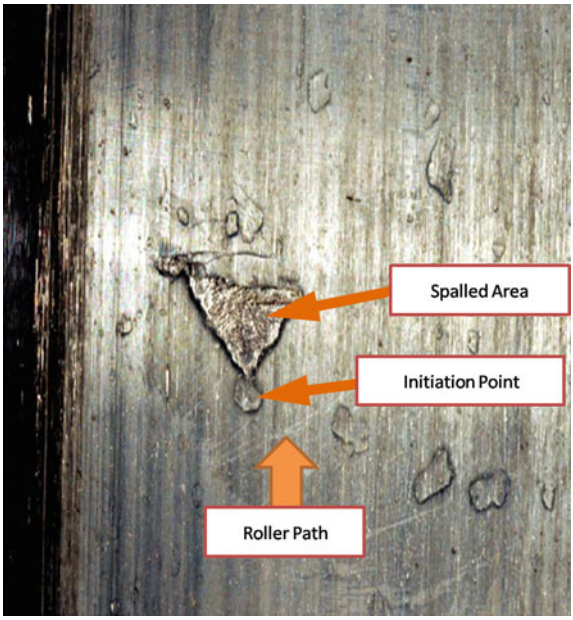

Fig. 18.24 New spall formed on inner raceway of a wind turbine roller bearing. With continued operation the spall would rapidly grow and peel off the entire raceway surface. (From [89])

18.6.1.1 Surface-Initiated Fatigue Spalling

The dynamic clearances between moving parts are on the order of 1 μm, which is the same dimension as many hard contaminant particles. Hard particles trapped in rolling contacts indent raceway surfaces creating raised metal shoulders that act as stress risers [85–88]. The pressure increase around a dent can surpass the normal Hertzian pressure. During subsequent rolling cycles, tangential surface stress plus lubricant forced into the cracks cause the cracks to propagate beneath the surface. Cracks eventually undermined raceway surfaces, creating a fatigue spall (Fig. 18.24) in a similar manner as that described in Sect. 18.5.1.2. Copious quantities of wear-hardened steel are thus released as wear debris, which can lead to secondary damage if not quickly removed. As indicated by Fig. 18.25, hard ductile steel particles (including gear wear debris) are the most damaging. However, large quantities of any hard particle will seriously degrade the bearing life. This makes the wind turbine gearbox a severe application for bearing survival if contamination is not properly managed.

As cracks propagate within the steel, chemically reactive metal is exposed at newly opened crack tips. Dissolved water carried by the lubricant to these crack tips dissociates into its component chemical elements, hydrogen and oxygen gas (H_2 and O_2). The oxygen reacts with both lubricant and steel surfaces. Because hydrogen is the smallest possible molecule, it easily diffuses into grain boundaries where it weakens the steel by hydrogen embrittlement. This accelerates crack propagation and shortens the time to spall formation and component failure.

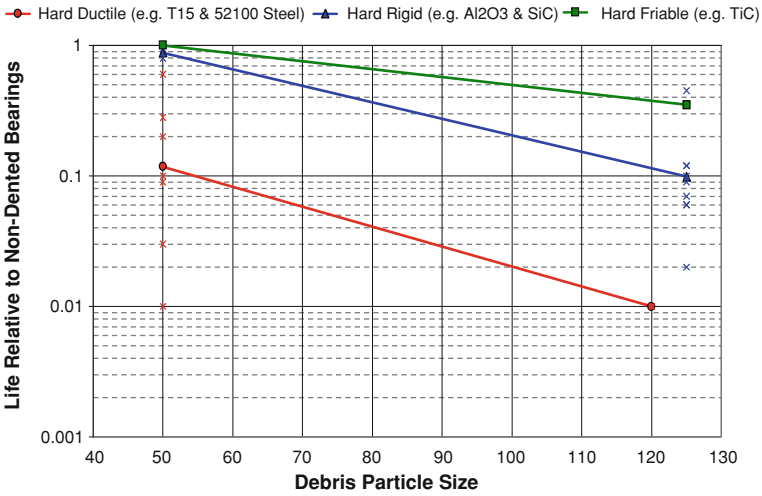

Fig. 18.25 Hard ductile particles, such as gear tooth wear debris, produce the greatest decrement to bearing life. More fragile particles tend to shatter in contact zone and produce less damage per particle. However, damage also increases with concentration for any type of hard particle contaminant [90]

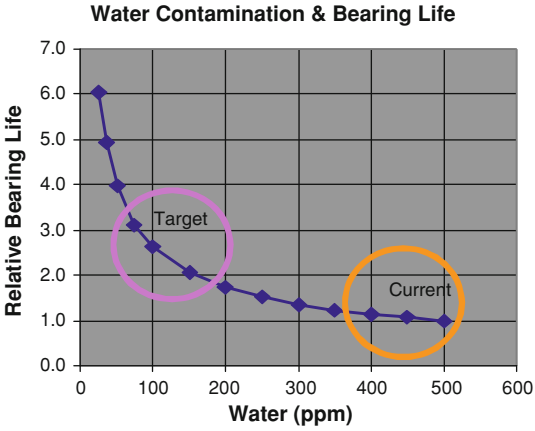

Fig. 18.26 Dissolved water and bearing life. Saturation level of water in oil is 500 ppm. Bearings operating in oil with *lower* levels of dissolved water have longer life. 'Current' refers to typical water contamination levels in wind turbine gearboxes; 'Target' refers to 125 ppm water level achieved through improved contamination control. (Original data from [91], and revised in [92])

Figure 18.26 shows decreasing bearing life as the concentration of dissolved water increases.

18.6.1.2 Abrasive Wear

Hard particles in sliding contacts (such as between gear teeth and in journal bearings) plough through and cut away component surfaces, resulting in frictional losses, elevated oil temperature, loss of fit and tolerance, and reduction in power transmission efficiency. The major offenders are abrasives used in manufacturing and gritty airborne minerals such as silica dust.

Table 18.4 Effects of metals and water on oil oxidation. Adapted from [93]

Condition	Hours (h)	TAN increase
Clean and dry	3,500	0.17
Iron	3,500	0.65
Copper	3,500	0.79
Water	3,00	0.80
Water + Iron	500	8.1
Water + Copper	40	11.2

18.6.1.3 Oil Oxidation

Because of difficulty, expense, and safety issues, wind turbine operators strive to minimize the frequency of gear oil changes. The enemy is oil degradation, which includes loss of additives, excessive accumulations of fine particles, and especially oil oxidation. This well-documented oxidation mechanism starts when oxygen atoms are incorporated into oil molecules producing chemically reactive free radicals, which in turn initiate chain reactions involving thousands of oil molecules and producing acids and polymeric compounds. The acids promote corrosion. The polymers are gummy substances that: (1) thicken the oil, fostering filter bypassing and lubricant starvation during cold starts, (2) foul passages and flow controls, another source of lubricant starvation, and (3) coat and thermally insulate heat exchange surfaces, fostering excessive heat build-up and elevated temperatures during operation.

Antioxidants (free-radical scavengers) are incorporated into gear oil additive packages to intercept the free radicals and terminate the chain reaction. When the antioxidant additives become depleted, oxidation takes over, and the degraded oil requires replacement. A strategy for extending oil life and oil change intervals is to reduce the rate of depletion of antioxidant additives. This is accomplished by: (1) keeping the oil cool, (2) inhibiting the generation of metal wear debris and sequestering fresh debris away from hotter zones, and (3) keeping water levels below 100–200 ppm. Regarding temperature, the rate of oil oxidation tends to follow the simple, yet reliable, estimation for oil temperature: The rate of a chemical reaction approximately doubles for every 10°C increase in temperature. Maintaining gear oil operating temperature below ~50°C will alleviate most oxidation issues due to hot oil.

The surfaces of fresh metal wear particles are catalytic, promoting the formation of free radicals and accelerating oil oxidation. As summarized in Table 18.4, one classic study found fresh metal surfaces accelerated oxidative oil degradation by 6–8 times, as measured by increasing *Total Acid Number* (TAN) values. Per unit surface area, copper was the worst offender (such as from tubing and bronze bushings). However, the greater amounts of iron-containing wear debris found in gearboxes are likely the major offenders for wind turbines. In the same study, water by itself was found to accelerate oil oxidation as rapidly as copper. However, water together with either copper or iron accelerated the rate of oil oxidation by a factor of 300.

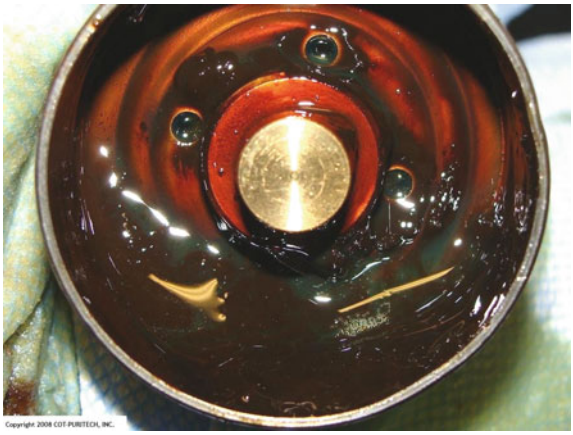

Fig. 18.27 Water-induced additive drop-out fouling a gearbox thermostat, rendering it inoperative (COT-Puritech, Inc.)

18.6.1.4 Hydrolysis

In addition to oxidation, wind turbine gear oils can degrade through the direct hydrolysis of ester-based additives. These types of additives are synthesized by reacting alcohols and acids to produce the required esters, along with water as a by-product. In operating systems, dissolved water drives the reaction in reverse, decomposing esters back into alcohols (mostly innocuous) and acids (quite harmful), along with depletion of the ester-based additives. Acids produced by hydrolysis promote corrosion and can also react with metals to produce fouling gels.

18.6.1.5 Additive Drop-Out

Another form of oil degradation is additive drop-out. Some gear oil additives have strong affinity for water (hydrophilic polar additive molecules). They become unavailable by congregating in and around water droplets. Furthermore, high concentrations of dissolved water can break colloidal suspensions of finely divided powders sometimes used as anti-wear additives, resulting in dumping of massive amounts of material. Not only are these additives inactivated by water, but as illustrated in Fig. 18.27, additive drop-outs can completely foul components and make them inoperable.

18.6.1.6 Corrosion

Galvanic corrosion requires current of ions in aqueous solution, and therefore the presence of free water. Even a thin film of water suffices. NaCl salt accelerates the corrosion of metals, making offshore and coastal marine environments especially

sensitive to this wear mode. Corrosion results in pitting, leakage, weakening, and breaking of parts, and release of abrasive particles into the oil (such as iron oxide, better known as rust).

18.6.1.7 Microbial Growth

To grow and multiply microbes need three requirements: moderate temperatures, food, and free water. Many strains of bacteria and molds will metabolize gear oil. If free water is present along with temperatures ranging from 15 to 52°C (60–125 F), these will thrive. Consequences include accumulation of acids (promoting corrosion since free water is present), and the formation of biological slimes that foul flow passages and moving parts. Microbial colonization of lubricants is also associated with fetid odors, asthma, and skin allergies.

18.6.2 Contamination Control

Strategies for ameliorating the harmful effects of oil contamination have been developed over the past 40 years in the construction, mining, agriculture, and aerospace industries, and some of the knowledge gained is currently being applied to the wind turbine industry. Some of the practices that are currently being recommended for the manufacture, assembly, and maintenance of wind turbines are listed in Table 18.5.

Additionally, an appropriately designed oil filtration system is critical for minimizing the possibility of early gear or bearing failure. Most wind turbines incorporate one or more filtration systems to remove debris and contaminants from the lubricant. Inline filters, which are placed within the same circulation line as the delivery system, are now standard on most current turbines. To keep the gear oil cool, a heat exchanger is used prior to returning the filtered oil back to the gearbox, typically keeping the maximum oil temperature below 70°C [94]. Some turbines are also designed with an offline or bypass filtration system. These systems include a separate pump that circulates oil through an independent filter. Figure 18.28 depicts a typical contamination control system, complete with a water absorption filter. Offline particle filters are needed only if online filters are insufficient to maintain lubricant cleanliness.

18.6.2.1 Rating Particle Filters

The international standard method for rating lube and hydraulic filters is the Multi-Pass Test [95]. As illustrated in Fig. 18.29, a slurry of silica particles is continuously fed into the test circuit. As particles flow into the filter under test, some are captured, and the remainder continues to recirculate. Throughout the

Table 18.5 Summary of recommended contamination control practices for wind turbines

Area	Description
Design	Drain oil from gears directly back into the sump, bypassing bearing packages. This allows filters to remove gear wear debris upstream of bearings. Use dynamic seals with minimal breathing
Materials	Avoid brittle materials that can shed hard particles. Avoid copper containing alloys contacting lubricants
Component and subsystem cleanliness	Remove manufacturing swarf, grinding/polishing compounds, machine chips, airborne dirt. Avoids early damage leading to premature failures. See ISO 10949
Roll-off cleanliness	Systems and replacement parts should be shipped in cleaner condition than operating systems
Transportation	Ship in sealed packaging to prevent ingression of airborne dust and water from rain and splashing
On-site storage	Seal and store systems and replacement parts in protected enclosures
Prevent contaminant ingression	Install regenerable breather dryers and/or pressured dry air blankets
Rapid contaminant removal	Install 5 μm full-flow (inline) particle filters
Off-line contaminant removal	Install water removing cartridges offline; use dry air blanket systems as needed. If 5 μm full-flow filters not available, supplement with 3 μm offline filters

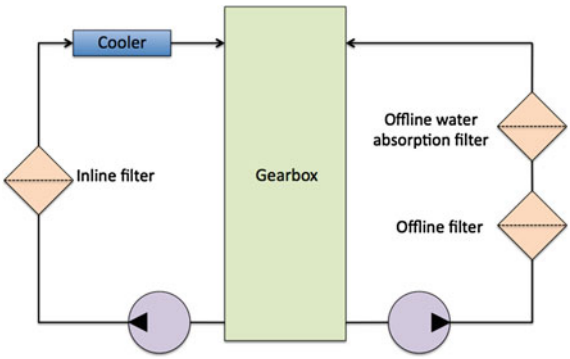

Fig. 18.28 Flowchart of a contamination control system

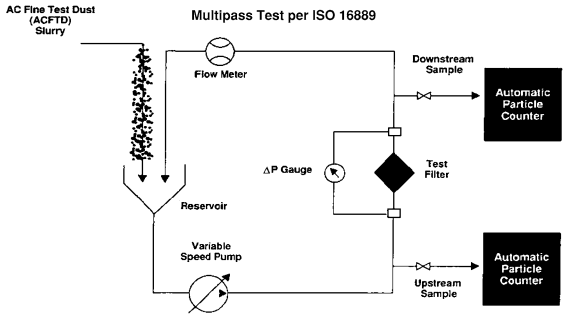

Fig. 18.29 Schematic of the multi-pass test for rating filter efficiency. A fine powder of contaminant, ISO medium test dust, is continuously fed into the system. Upstream and downstream particle counts taken during the test are used to calculated the beta value ($\beta_{X(C)}$), as described in the text

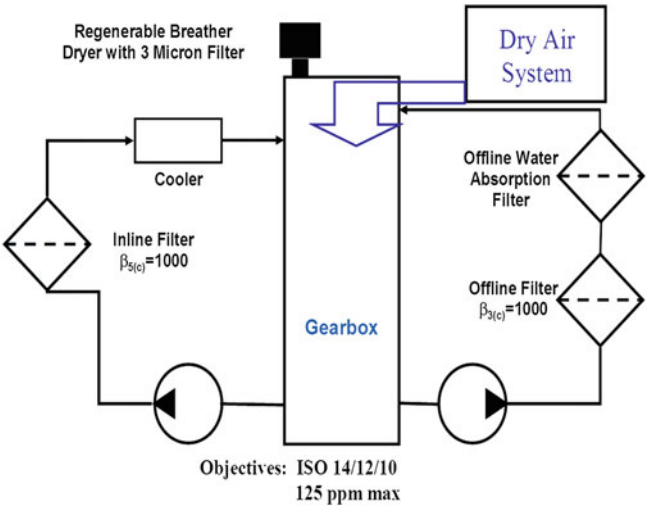

Fig. 18.30 Detailed diagram of recommended filtration cycle for ingression prevention and removal. Main lubricant circuit on *left*, with 5 μm ($\beta_{5(C)} \geq 1{,}000$) installed. Side-loop (offline) circuit shown with optional 3 μm ($\beta_{3(C)} \geq 1{,}000$) particle filter and water absorbing cartridge. Also shown is optional dry air system for removing water from gear oil [96]

test, the number of upstream and downstream particles is measured with electronic automatic particle counters. Filter efficiency for particle size X (in microns) is reported as the ratio of upstream to downstream counts recorded during the test. This measure of filter efficiency is termed the 'beta ratio', $\beta_{X(C)}$:

$$\beta_{X(C)} = (\text{Upstream Counts } \geq X\mu\text{m}) \div (\text{Downstream Counts } \geq X\mu\text{m}) \quad (18.24)$$

Modern filter ratings are $\beta_{X(C)} \geq 200$ and $\beta_{X(C)} \geq 1000$. As an example, for a filter rated at $\beta_{5(C)} = 1{,}000$, 1 out of every 1,000 particles equal to or greater than 5 μm passed through the filter during the test, while the other 999 particles were captured by the filter.

18.6.2.2 Recommended Oil Particle Filters

A detailed model of a wind turbine contamination control system is shown in Fig. 18.30. When available, full-flow filters rated at $\beta_{5(C)} \geq 1{,}000$ are recommended. As shown in Fig. 18.31, bearing life can be extended 2–5 times simply by installing 5 μm full-flow gear oil filters in place of the older, less-efficient 10–25 μm filters found in some wind turbine gearboxes. In addition, wear debris released by gear teeth, bushings, and some dynamic seals are diminished in clean oil maintained by 5 μm filters, resulting in less abrasive wear. Full-flow filters also capture catalytic fresh metallic wear debris before passing into hot sections of the gearbox, reducing the rate of oil oxidation and extending oil life.

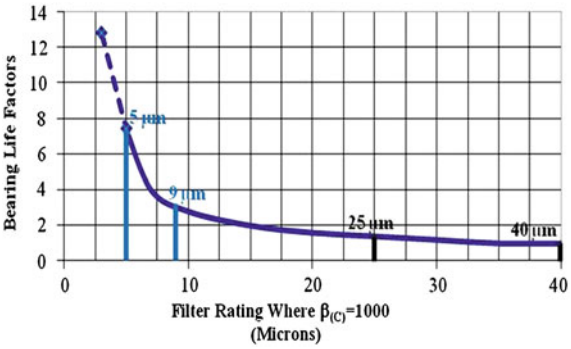

Fig. 18.31 Bearing life factors as a function of filter ratings (Original life factors in [97], revised to reflect changes in filter rating method by [98].)

A difficulty with older types of high-efficiency full-flow filters is excessive flow restriction (i.e., large pressure drop across the filter). This can be especially demanding when filtering high viscosity wind turbine gear oils. However, this problem has been solved with the introduction of a new generation of filters using bi-component fiber technology [99]. As illustrated in Fig. 18.32, replacing resin binders that film over and occlude pores with fibers that reinforce the porous structure results in filter media that is stronger, thinner, more open, and less flow restricting. As summarized in Table 18.6, new-generation 5 µm full-flow filters ($\beta_{5(C)} \geq 1{,}000$) installed into standard housings have maintained wind turbine gear oils consistently cleaner than the best conventional wind turbine gearbox filters, and have service lives greater than 12 months.

When 5 µm full-flow filters ($\beta_{5(C)} \geq 1000$) are not available for a particular model gearbox, then 10 µm or coarser filters are installed. In these cases high efficiency offline (a.k.a. side-loop) filters may be considered to supplement the coarser full-flow filter. It is recommended that offline filters have a rating of 3 or 5 µm ($\beta_{3(C)}$ or $\beta_{5(C)} \geq 1{,}000$), depending on the recommendation of the oil suppliers. Offline filter circuits require their own pump and source of power, and typically are kept on continuously. Because they function at very low rates of flow, typically 1/20 or less of full-flow, offline filters do not remove particles fast enough to protect against recent ingressions of hard particles. They can help maintain oil cleanliness by slowly removing the particles 5 µm and smaller that coarser full-flow filters cannot.

18.6.2.3 Recommended Air Breathers

To prevent ingression of abrasive airborne particles, vents should be equipped with air breathers capable of removing particles as small as 1 µm. Because vents also provide pathways for humidity to pass into gearboxes, these breathers typically combine an air particle filter and a humidity remover, as described below.

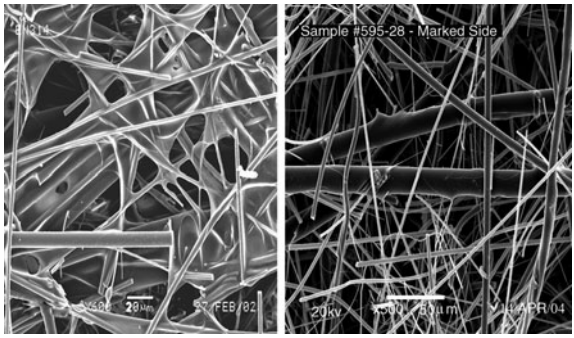

Fig. 18.32 Scanning electron photomicrographs of two types of 5 μm filter media. In conventional media on *left*, flow channels occluded by binder resin filming *over* microglass fibers. On *right*, unobstructed flow passages in bi-component media held together by larger binder fibers to which microglass fibers adhere, resulting in *lower* flow restriction (ΔP) and greater dirt holding capacity

Table 18.6 Polyalphaolefin-based gear oils from three different manufacturers. Filter rating X based on $\beta_{X(C)} \geq 1000$, per ISO 16899 [99]

Gear oil	Filter type (μm)	ISO averages
A	10	19/16/13
	5	17/15/12
B	10	21/17/13
	5	19/16/12
C	10	21/18/13
	5	19/16/11

18.6.3 Water Control

Component life can be significantly extended by keeping gear oil dry. For example, as shown in Fig. 18.31, compared to typical water contamination levels of 400–500 ppm found in many wind turbine gearboxes, maintaining gear oil near ~125 ppm increases bearing life two to three times.

Two approaches are normally used for minimizing water contamination in operating wind turbines:

- *Minimize humidity ingression through vents*: Ingression is minimized by installing vent breathers that prevent humidity from passing into the gearbox. Older types of desiccant breathers using silica gel are effective. However, these types of units have low water holding capacity, resulting in short service lives on the order of weeks to days in humid environments. This problem is avoided by installing regenerable breather driers on vents. These units have unlimited service life with respect to water. As illustrated in Fig. 18.33, humidity is removed from incoming air during the inhalation phase by thin-film adsorption; then during exhalation the unit regenerates by releasing and returning the previously captured water back into the atmosphere.

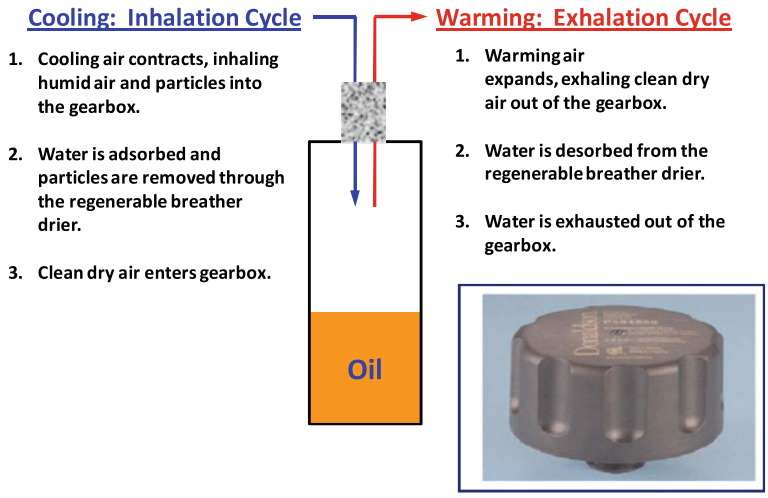

Fig. 18.33 The regenerable breather dryer (*inset*) contains a thin film of adsorbent distributed *over* a large porous surface area, as well as a fine air particle filter. During inhalation water vapor and airborne particles are removed and prevented from entering the system. During start-up air warms inside the reservoir, reducing its relative humidity. During exhalation water vapor retained by the thin film desorbs back into the warmed air and passes back to the environment [100]

Fig. 18.34 At time zero emulsified water injected into oil to 11,000 ppm (1.1%) free water concentration. Oil then recirculated through a single water absorbing cartridge at a turnover rate of 1 every 6 min. All free water removed in 12 turnovers. Saturation level of dissolve water in this oil = 200 ppm. (Turnover rate = fluid volume/flow rate)

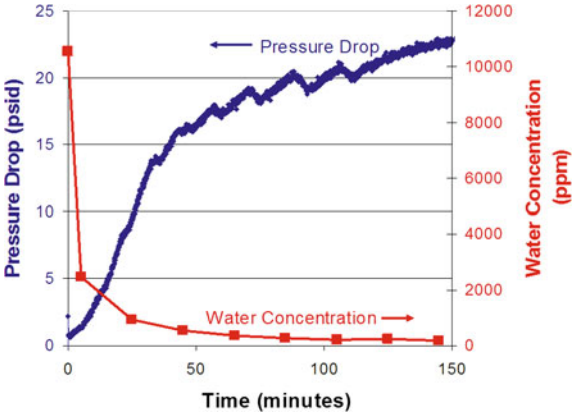

Water may also enter wind turbine gearboxes during maintenance activities or through external seals. A recommended practice for removing this water is to install a water absorbing cartridge in the off-line position. Externally these units appear similar to particle filters, but inside have quite different constructions. Some are made from porous cellulose-based materials with limited rates of removal and water holding capacity. Preferred units incorporate super-absorbent polymers (SAP) with 95% water removal efficiency that rapidly take out free water and also a portion of the dissolved water, as shown in Fig. 18.34.

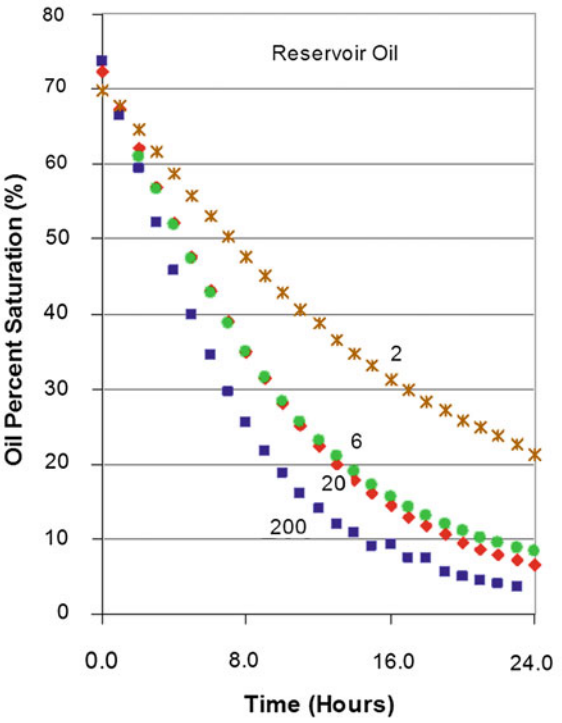

Fig. 18.35 Drying oil with a dry air blanket. Low flow of very dry air (−40°C dew point) sweeps *over* surface of oil in reservoir, bringing oil to less than 20% saturation (<100 ppm for most gear oils). Values on graph indicate the number of headspace turnovers per hour [100]

Finally, a proven technology known as *dry air blankets* has recently been adapted to wind turbines for water contamination removal. In this system, compressed air passes through a pressure swing absorber producing very dry air (−40°C dew point). Flow is arranged so that a blanket of the dry air sweeps over the oil surface in the reservoir. Gear oil is continuously dehumidified by contacting the dry air, as shown in Fig. 18.35. Slight pressurization of the system also inhibits ingression of humid air. Thus dry air blankets minimize water ingression and simultaneously remove water from gearboxes.

18.7 Condition Monitoring

Wind turbine condition monitoring systems allow early warnings of mechanical and electrical faults, which allow the operator to plan system repair before severe failure takes place [101]. Because early damage to components can oftentimes be detected while the turbine is still operational, repair work can be planned well in advance. This is considered to be of importance particularly in regard to offshore wind turbines, where bad weather conditions can prevent repair actions for several weeks [3]. Typical wind turbine sensors include those for measuring the following: (1) rotor position and speed, (2) generator position and speed, (3) power output,

(4) tower vibrations and deflections, (5) blade deformations, and (6) controller inputs such as pitch and yaw settings [102].

Condition monitoring can be performed in one of two ways, namely:

- *Offline*: Not to be confused with offline filtration as described in Sect. 18.6.2, this method involves periodic inspections that require the turbine to be shut down, and may also require the attention of an operator. This method may also incorporate the use of diagnostic equipment.
- *Online*: This method involves the use of automated sensory equipment that monitor the components in the turbine continuously during operation. The system may report raw measurements (stress, deflection, etc.), or may also incorporate processing systems for data analysis.

Condition monitoring techniques that pertain to the tribological condition of the system, namely vibration analysis and oil analysis, are described in the following sections.

18.7.1 Vibration Analysis

Vibration sensing is one of the most well-known methods for monitoring the condition of gears and bearings. The sensors that are commonly used depend on the frequency range that is to be measured, according to the following:

- Position transducers for monitoring low-frequency vibrations
- Velocity transducers for monitoring middle-frequency vibrations
- Accelerometers for monitoring high-frequency vibrations
- Spectral emitted energy (SEE) sensors for very high-frequency vibrations

Additionally, specialized offline acoustic monitoring can be used to determine the presence of cracks or defects in wind turbine components. Monitoring of this sort involves the attachment of acoustic sensors directly onto the component using glue with low attenuation, which then monitor the acoustic frequency of the component. The monitoring can take place either passively (i.e., the excitation is generated by the component itself), or actively (i.e., the excitation is externally applied).

18.7.2 Oil Analysis

Oil analysis can provide information about the health of gears and bearings, as well as detect the presence of particulate or water contamination. For turbines that are monitored offline, experience has shown that oil analysis should be performed after every 4,000 h of operation. After taking a sample of oil from the gearbox, analyses that are commonly performed include:

- *Oxidation*: By analyzing the visual appearance of the used lubricant, one can determine whether it is oxidized. Ideally, the lubricant should appear clear and bright; lubricant-darkened colors may indicate oxidation. Also, the odor of lubricant can be analyzed, in that a sour, pungent, or "burnt" smell indicates that oxidation has taken place. Finally, a measure of the lubricant viscosity may allow for the determination of oxidation, as an increase in viscosity over that of fresh oil can be caused by oxidative effects.
- *Water Content*: Water contamination can be determined by a *crackle* test (i.e., placing the oil on a hot plate to determine the degree of bubble formation), or by more sophisticated methods, such as distillation, infrared, and Karl Fischer analysis.
- *Particulate Contamination*: Similar to the oxidation test, the visual appearance of lubricant (i.e., darkened colors), as well as an increase in the lubricant viscosity, may also indicate particulate contamination. More sophisticated methods such as spectrochemical analysis and automatic particle counting can provide significant details as to the size and composition of contaminants.

Although offline oil analysis is frequently used, an increasing number of wind turbine systems are being equipped with online oil monitoring systems which provide continuous monitoring of a small fraction of the lubricant. These systems may rely on optical, electromagnetic, or other physical principles to sense the degree of particle contamination. It must also be noted that a specialized class of lubricant monitoring, denoted as inline monitoring systems, involves the monitoring of all of the circulating fluid [57].

18.8 Closure

Wind turbine designs have evolved significantly since their inception and all indications point to continued growth in both installation rate and technological development. Wind turbines incorporate a number of tribological systems, including low-speed, intermediate-speed, and high-speed drivetrain gears and bearings, oscillatory pitch and yaw bearings, and a mechanical brake. As increasingly powerful wind turbines have been designed over the years, more attention has been paid towards solving the tribological challenges in wind turbine systems, although many challenges remain. In particular, advanced filtration technology is of upmost importance, as clean lubricant is crucial towards maximizing the lifetime of critical drivetrain components. It is also important to have a detailed understanding of the loads that are being applied to wind turbine tribological systems. Having this knowledge will aid in the selection of the most appropriate tribological component for each section of the turbine, and will also allow for reasonable estimations of the failure lifetime of each component. Finally, condition monitoring is important for monitoring the health of tribological components.

Wind turbine manufacturers are trending towards developing wind turbines of increasingly larger size and power capacity. This is especially the case for offshore

wind turbine power plants where the wind loads are complex and highly variable. To ensure the reliability of extra-large-scale turbines, it is important to have robust designs of the tribological systems as well as sufficient filtration and online condition monitoring to make the system less reliant on routine checkups and maintenance.

References

1. B.C. Babu, K.B. Mohanty, Doubly-fed induction generator for variable speed wind energy conversion systems–modeling and simulation. Int. J. Comput. Electr. Eng. **2**(1), 141–147 (2010)
2. H. Chandler (ed.), *Wind Energy–The Facts, in European Wind Energy Association* (2003)
3. Y. Amirat, M.E.H. Benbouzid, B. Bensaker, R. Wamkeue, *Condition Monitoring and ault Diagnosis in Wind Energy Conversion Systems: A Review in Electric Machines and Drives Conference. IEMDC '07, IEEE International*, 2007
4. Global Wind 2009 Report, Global Wind Energy Council, 2010
5. 20% Wind Energy by 2030, U.S. Department of Energy Technical Report, 2008
6. Strategic research agenda: market deployment strategy from 2008 to 2030, European Wind Energy Technology Platform, 2008
7. Mid and long range plan for renewable energy development, Chinese Committee for National Development and Reform, 2007
8. B. Lu, Y. Li, X. Wu, Z. Yang, in *A review of recent advances in wind turbine condition monitoring and fault diagnosis* (Power Electronics and Machines in Wind Applications, PEMWA, IEEE, 2009), pp. 1–7
9. 2009 wind technologies market report, U.S. Department of Energy, 2010
10. J. Ribrant, L. Bertling, Survey of failures in wind power systems with focus on Swedish wind power plants during 1997–2005. IEEE Power Engineering Society General Meeting, 2007
11. E.J. Terrell, W.M. Needelman, J.K. Kyle, Current and future tribological challenges in wind turbine power systems, in *STLE/ASME international joint tribology conference*, ASME IJTC2009-15220, 2009
12. Wind Energy Siting Handbook, American Wind Energy Association, 2008
13. L. Mumper, Wind turbine technology turns on bearings and condition monitoring. Utilities Manager, 2006
14. M. Islam, D.S.K. Ting, A. Fartaj, Aerodynamic models for Darrieus-type straight-bladed vertical axis wind turbines. Renew. Sustain. Energy Rev. **12**(4), 1087–1109 (2008)
15. A.C. Hansen, C.P. Butterfield, Aerodynamics of horizontal-axis wind turbines. Annu. Rev. Fluid Mech. **25**(1), 115–149 (1993)
16. S. Oerlemans, P. Sijtsma, B. Méndez López, Location and quantification of noise sources on a wind turbine. J. Sound Vib. **299**(4–5), 869–883 (2007)
17. A.D. Hansen, L.H. Hansen, Wind turbine concept market penetration over 10 years (1995–2004). Wind Energy **10**, 81–97 (2007)
18. L.H. Hansen, L. Helle, F. Blaabjerg, E. Ritchie, S. Munk-Nielsen, H. Binder, P. Soerensen, B. Bak-Jensen, Conceptual survey of generators and power electronics for wind turbines. Riso National Lab Technical Report, 2001
19. T. Burton, D. Sharpe, N. Jenkins, E. Bossanyi, *Wind Energy* (Wiley, NY, 2001)
20. A. Petersson, *Analysis, modeling and control of doubly-fed induction generators for wind turbines*, in *Department of Energy and Environment*, Chalmers University of Technology, 2005
21. H. Li, Z. Chen, Overview of different wind generator systems and their comparisons. Renew. Power Gener. IET **2**(2), 123–138 (2008)
22. H. Polinder, F.F.A. van der Pijl, G.J. de Vilder, P.J. Tavner, Comparison of direct-drive and geared generator concepts for wind turbines. Energy conversion. IEEE Trans **21**(3), 725–733 (2006)

23. G.L. Johnson, *Wind Energy Systems* (Prentice-Hall, Englewood Cliffs, 1985)
24. D.S. Zinger, E. Muljadi, Annualized wind energy improvement using variable speeds. IEEE Trans. Indus. Appl. **33**(6), 1444–1447 (1997)
25. S.A. Akdag, Ö. Güler, Comparison of wind turbine power curve Models, in *International Renewable Energy Congress*, Sousse, Tunisia, 2010
26. C. Zhe, J.M. Guerrero, F. Blaabjerg, A review of the state of the art of power electronics for wind turbines. Power Electron. IEEE Trans. **24**(8), 1859–1875 (2009)
27. J. Peeters, *Simulation of Drive Train Loads in a Wind Turbine* (Katholieke Universiteit Leuven, Lueven, 2006)
28. E. Hau, *Wind Turbines* (Springer-Verlag, Berlin, 2006)
29. W. Musial, S. Butterfield, B. McNiff, Improving wind turbine gearbox reliability, in *Proceedings of the European Wind Energy Conference*, Milan, Italy, 2007
30. H. Slootweg, E. De Vries, Inside wind turbines-fixed vs variable speed. Renew. Energy World **6**(1), 3041 (2003)
31. American Gear Manufacturer's Association, Standard for design and specification of gearboxes for wind turbines, ANSI/AGMA/AWEA 6006-A03, 2004
32. H. Stiesdal, *The Wind Turbine Components and Operation* (Bonus-Info, Denmark, 1999)
33. K.L. Johnson, *Contact Mechanics* (Cambridge University Press, Cambridge, 1985)
34. D.H. Buckley, *Surface Effects in Adhesion, Friction, Wear, and Lubrication* (Elsevier, Amsterdam, 1981)
35. M.N. Kotzalas, G.L. Doll, Tribological advancements for reliable wind turbine performance. Philos. Trans. Royal Soc. A: Math. Phys. Eng. Sci. **368**(1929), 4829–4850 (2010)
36. T.A. Harris, M.N. Kotzalas, *Essential Concepts of Bearing Technology* (Taylor and Francis, Boca Raton, 2007)
37. K. Iso, A. Yokouchi, H. Takemura, Research work for clarifying the mechanism of white structure flaking and extending the life of bearings. in SAE Technical Paper 2005-01-1868, Society of Automotive Engineers, 2005
38. M. Kohara, T. Kawamura, M. Egami, Study on mechanism of hydrogen generation from lubricants. Tribol. Trans. **46**, 5360 (2006)
39. A.V. Olver, The mechanism of rolling contact fatigue: an update. J. Eng. Tribol. **219**(5), 313–330 (2005)
40. G. Lundberg, A.Z. Palmgren, Dynamic capacity of rolling bearings. Proc. R. Swed. Acad. Eng. Sci. **196**, 50 (1947)
41. E.V. Zaretsky, Palmgren revisited–a basis for bearing life prediction. Lubr. Eng. **54**, 1823 (1998)
42. F.T. Barwell, Report on papers in Session 3 (lubrication), in *Proceedings of the International Conference on Gearing* (1958), pp. 23–25
43. D. Dowson, G.R. Higginson, *Elastohydrodyanmic Lubrication*, 2nd edn. (1977)
44. A.N. Grubin, *Investigation of the Contact of Machine Components* (Central Scientific Research Institute for Technology and Mechanics, Moscow, 1949), Book 30
45. R.D. Britton, C.D. Elcoate, M.P. Alanou, H.P. Evans, R.W. Snidle, Effect of surface finish on gear tooth friction. J. Tribol. **122**(1), 354–360 (2000)
46. A.N. Grubin, *Fundamentals of the hydrodynamic theory of lubrication of heavily loaded cylindrical surfaces*. Investigation of the Contact Machine Components, No. 30, 115–166 (1949)
47. D. Dowson, G.R. Higginson, A numerical solution to the elasto-hydrodynamic problem. J. Mech. Eng. Sci. **1**(1), 6–15 (1959)
48. D. Dowson, G.R. Higginson, *Elastohydrodynamic Lubrication* (Pergamon Press, Oxford, 1977)
49. S. Li, A. Kahraman, Prediction of spur gear mechanical power losses using a transient elastohydrodynamic lubrication model. Tribol. Trans. **53**, 554–563 (2010)
50. R. Gohar, *Elastohydrodynamics* (Wiley, New York, 1988)
51. R. Errichello, Friction, lubrication, and wear of gears, in *ASM Handbook Friction, Lubrication, and Wear Technology*, vol. 18, ed. by P. Blau (ASM International, Materials Park, Ohio, 1992), pp. 535–545

52. T.E. Tallian, Simplified contact fatigue life prediction model–part I: review of published models. J. Tribol. **114**(2), 207–213 (1992)
53. G. Stachowiak, A.W. Batchelor, *Engineering Tribology* (Elsevier, Oxford, 2005)
54. G.L. Doll, B.K. Osborn, Engineering surfaces of precision steel components. Proc. Annu. Tech. Conf. Soc. Vac. Coaters **44**, 78–84 (2001)
55. G.L. Doll, C.R. Ribaudo, R.D. Evans, Engineered surfaces for steel rolling element bearings and gears. Mater. Sci. Technol. **2**, 367–374 (2004)
56. A. Ragheb, M. Ragheb, Wind turbine gearbox technologies, in *International Nuclear and Renewable Energy Conference* (*INREC10*) (Amman, Jordan, 2010)
57. R.W. Hyers, J.G. Mcgowan, K.L. Sullivan, J.F. Manwell, B.C. Syrett, Condition monitoring and prognosis of utility scale wind turbines. Energy Mater.: Mater. Sci. Eng. Energy Syst. **1**(3), 187–203 (2006)
58. F.L. Litvin, A. Fuentes, *Gear Geometry Applied Theory* (Cambridge University Press, Cambridge, 2004)
59. J.E. higley, *Mechanical Engineering Design* (McGraw-Hill, New York, 1963)
60. P. Lynwander, *Gear Drive Systems: Design and Application* (Marcel Dekker, NY, 1983)
61. F.L. Litvin, A. Fuentes, I. Gonzalez-Perez, L. Carvenali, K. Kawasaki, R.F. Handschuh, Modified involute helical gears: computerized design simulation of meshing and stress analysis. Comput. Methods Appl. Mech. Eng. **192**(33–34), 3619–3655 (2003)
62. J. Kleemola, A. Lehtovaara, Experimental simulation of gear contact along the line of action. Tribol. Int. **42**, 1453–1459 (2009)
63. G.M. Maitra, *Handbook of Gear Design* (Tata McGraw-Hill, New Delhi, 1997)
64. A.H. Elkholy, Tooth load sharing in high contact ratio spur gears. J. Mech. Trans. Autom. Des. **107**(1), 11–16 (1985)
65. S. Avinash, Application of a system level model to study the planetary load sharing behavior. J. Mech. Des. **127**(3), 469–476 (2005)
66. C.R.M. Rao, G. Muthuveerappan, Finite element modelling and stress analysis of helical gear teeth. Comput. Struct. **49**(6), 1095–1106 (1993)
67. B.R. Hohn, K. Michaelis, Influence of oil temperature on gear failures. Tribol. Int. **37**(2), 103–109 (2004)
68. H. Blok, Les temperatures de surface dans les conditions de graissage sons pression extreme, in *Second World Petroleum Congress*, Paris, 1937
69. E.E. Shipley, *Failure analysis of coarse-pitch, hardened, and ground gears*. Paper No. P229.26, (American Gear Manufacturers Association, Alexandria, 1982), pp. 1–24
70. S. Tanaka, *Appreciable increases in surface durability of gear pairs with mirror-like finish*, Paper No. 84-DET-223, (American Society of Mechanical Engineers, Alexandria, 1984), pp. 1–8
71. X. Ai, Effect of debris contamination on the fatigue life of roller bearings. Proc. Inst. Mech. Eng. Part J: J. Eng. Tribol. **215**(6), 563–575 (2001)
72. I. Allison, E. Hearn, A new look at the bending strength of gear teeth. Exp. Mech. **20**(7), 217–225 (1980)
73. J. Hiremagalur, B. Ravani, Effect of backup ratio on root stresses in spur gear design. Mech. Based Des. Struct. Mach.: Int. J. **32**(4), 423–440 (2004)
74. W. Lewis, Investigation of the strength of gear teeth, in *Proceedings of Engineers Club*(1892), pp. 16–23
75. T.J. Dolan, E.L. Broghamer, *A photoelastic study of stresses in gear tooth fillets*. University of Illinois Bulletin, vol 355 (1942)
76. B.W. Kelley, R. Pedersen, The beam strength of modern gear tooth design. Transactions of the S.A.E., 1957
77. X.Q. Peng, L. Geng, W. Liyan, G.R. Liu, K.Y. Lam, A stochastic finite element method for fatigue reliability analysis of gear teeth subjected to bending. Comput. Mech. **21**(3), 253–261 (1998)
78. J.D. Andrews, A finite element analysis of bending stresses induced in external and internal involute spur gears. J. Strain Anal. Eng. Des. **26**(3), 153–163 (1991)

79. M.A. Miner, Cumulative damage in fatigue. J. Appl. Mech. **67**, A159–A164 (1945)
80. A.Z. Palmgren, Die Lebensdauer von Kugelagern. 2 ver Deutsch Ing **68**, 339–341 (1924)
81. T.A. Harris, J.H. Rumbarger, C.P. Butterfield, Wind turbine design guideline DG03: yaw and pitch rolling bearing life, NREL Technical Report No. NREL/TP-500-42362, 2009
82. T. Senjyu, R. Sakamoto, N. Urasaki, T. Funabashi, H. Fujita, H. Sekine, Output power leveling of wind turbine generator for all operating regions by pitch angle control. IEEE Trans. Energy Convers. **21**(2), 467–475 (2006)
83. J. Aguirrebeitia, R. Aviles, I.F.d. Bustos, M. Abasolo, Calculation of general static load-carrying capacity for the design of four-contact-point slewing bearings. J. Mech. Des. **132**(6), P064501 (2010)
84. W.J. Bartz, Tribological aspects of wind power plants, in *Proceedings of the World Tribology Congress III*, Washington, D.C., USA, 2005
85. J.C. Enthoven, H.A. Spikes, Visual observation of the process of scuffing, in *Lubricants and Lubrication, Proceedings of the 21st Leeds-Lyon Symposium on Tribology* (1995), pp. 487–494
86. G.K. Nikas, R.S. Sayles, E. Ioannides, Effects of debris particles in sliding/rolling elastohydrodynamic contacts. J. Eng. Tribol. **212**(5), 333–343 (1998)
87. G. Xu, F. Sadeghi, J.D. Cogdell, Debris denting effects on elastrohydrodynamic lubricated contacts. Trans. ASME J. Tribol. **119**, 579–587 (1997)
88. X. Ai, H.S. Cheng, The influence of moving dent on point EHL contacts. Tribol. Trans. **37**(2), 323–335 (1994)
89. S. Butterfield, R. Errichello, B. McNiff, Wind turbine gearbox issues and lubrication, in *IJTC2008-71361*, 2008
90. M.N. Kotzalas, W.M. Needelman, D.R. Lucas, G.L. LaVallee, Improving wind turbine gearbox life, in *AWEA Windpower Conference*, Houston, 2008
91. R.E. Cantley, The effect of water in lubricating oil on bearing fatigue life. ASLE Trans. **20**(3), 244–248 (1977)
92. E.V. Zaretsky (ed.), *Life Factors for Rolling Bearings* (Society of Tribologists and Lubrication Engineers, Park Ridge, 1992)
93. E. Abner, in *Handbook of Lubrication*, ed. by E.R. Booser, Lubricant deterioration in service (CRC Press, Boca Raton, 1983)
94. W.M. Needelman, M.A. Barris, and G.L. LaVallee, Contamination Control for Wind Turbine Gearboxes. Power Engineering
95. Hydraulic fluid power—Filters—Multi-pass method for evaluating filtration performance of a filter element. ISO 16889. 2008: International Organization for Standardization
96. W.M. Needelman, M.A. Barris and G.L. LaVallee, Contamination control for wind turbine gearboxes. Power Engineering, 2009
97. W.M. Needelman, E.V. Zaretsky, New equations show oil filtration effect on bearing life. Power Transm. Des. **33**(8), 65–68 (1991)
98. W.M. Needelman, E.V. Zaretsky, Recalibrated equations for determining effect of oil filtration on rolling bearing life, in *STLE Annual Meeting*, Orlando (2009)
99. W.M. Needelman, M.A. Barris, G.L. LaVallee, Reducing cost of operation in harsh conditions with new generation filters, in *International Fluid Power Exposition*, Las Vegas (2011)
100. G.L. LaVallee, W.M. Needelman, Dry air blankets: An effective and economical method for eradicating water contamination. Part I: principles of operation, in *STLE Annual Meeting*, Las Vegas (2010)
101. C.S. Gray, S.J. Watson, Physics of failure approach to wind turbine condition based maintenance. Wind Energy **13**(5), 395–405 (2010)
102. Z. Hameed, Y.S. Hong, Y.M. Cho, S.H. Ahn, C.K. Song, Condition moitoring and fault detection of wind turbines and related algorithms: a review. Renew. Sustain. Energy Rev. **13**(1), 1–39 (2009)